HHS Public Access

Author manuscript

Oper Neurosurg (Hagerstown). Author manuscript; available in PMC 2017 March 01.

Published in final edited form as:

Oper Neurosurg (Hagerstown). 2016 March ; 12(1): 39–48. doi:10.1227/NEU.0000000000001033.

Magnetic Resonance Thermometry-Guided Stereotactic Laser Ablation of Cavernous Malformations in Drug-Resistant Epilepsy: Imaging and Clinical Results

D. Jay McCracken, M.D.[2,1], **Jon T. Willie, M.D., Ph.D.**[2,3,4,1], **Brad Fernald, M.S.**[5], **Amit M. Saindane, M.D.**[6], **Daniel L. Drane, Ph.D.**[3,7], **Daniel L. Barrow, M.D.**[2], and **Robert E. Gross, M.D., Ph.D.**[2,3,4,8]

[2]Department of Neurosurgery, Emory University School of Medicine, Atlanta, GA.

[3]Department of Neurology, Emory University School of Medicine, Atlanta, GA.

[4]Interventional MRI Program, Emory University Hospital, Atlanta, GA.

[5]Visualase, Inc., Houston, TX.

[6]Department of Radiology and Imaging Sciences, Emory University School of Medicine, Atlanta, GA.

[7]Department of Neurology, University of Washington School of Medicine, Seattle, WA.

[8]Coulter Department of Biomedical Engineering, Georgia Institute of Technology, Atlanta, GA.

Abstract

BACKGROUND—Surgery is indicated for cerebral cavernous malformations (CCM) that cause medically refractory epilepsy. Real-time magnetic resonance thermography (MRT)-guided stereotactic laser ablation (SLA) is a minimally invasive approach to treating focal brain lesions. SLA of CCM has not previously been described.

OBJECTIVE—To describe MRT-guided SLA, a novel approach to treating CCM-related epilepsy, with respect to feasibility, safety, imaging, and seizure control in 5 consecutive patients.

METHODS—Five patients with medically refractory epilepsy undergoing standard presurgical evaluation were found to have corresponding lesions fulfilling imaging characteristics of CCM and were prospectively enrolled. Each underwent stereotactic placement of a saline-cooled cannula containing an optical fiber to deliver 980-nm diode laser energy via twist drill craniostomy. MR anatomic imaging was used to evaluate targeting prior to ablation. MR imaging provided evaluation of targeting and near real-time feedback regarding extent of tissue thermocoagulation.

CORRESPONDING AUTHOR INFORMATION. Robert E. Gross, M.D., Ph.D., Department of Neurosurgery, Emory University School of Medicine, 1365 Clifton Road, NE, Suite 6200, Atlanta, GA 30322, rgross@emory.edu, Phone: 404-727-2354, Fax: 404-712-8576.

[1]These authors contributed equally to the preparation of this manuscript.

The terms of this arrangement have been reviewed and approved by Emory University in accordance with its conflict of interest policies.

CONTRIBUTIONS: DJM and JTW contributed equally to the data analysis, figure assembly, and writing of the manuscript. JTW and REG performed all surgical procedures. BF contributed to volumetric data analysis. AMS contributed to neurological imaging interpretation. DLD contributed to psychometric data analysis. REG conceptualized the study and edited the manuscript.

Patients maintained seizure diaries, and remote imaging (6–21 months post-ablation) was obtained in all patients.

RESULTS—Imaging revealed no evidence of acute hemorrhage following fiber placement within presumed CCM. MRT during treatment and immediate post-procedure imaging confirmed desired extent of ablation. We identified no adverse events or neurological deficits. Four of 5 (80%) patients achieved freedom from disabling seizures after SLA alone (Engel class 1 outcome), with follow-up ranging 12–28 months. Reimaging of all subjects (6–21 months) indicated lesion diminution with surrounding liquefactive necrosis, consistent with the surgical goal of extended lesionotomy.

CONCLUSION—Minimally invasive MRT-guided SLA of epileptogenic CCM is a potentially safe and effective alternative to open resection. Additional experience and longer follow-up are needed.

Keywords

Epilepsy; laser therapy; magnetic resonance imaging; minimally invasive surgical procedures; stereotactic techniques; cavernous malformation; thermometry

INTRODUCTION

Cerebral cavernous malformations (CCM) are a pathological lesion of the central nervous system consisting of mulberry-like, intertwined, thin-walled clusters of vascular sinusoids lined by endothelial cells without intervening parenchyma.[1] CCM have slow circulatory blood flow, making them angiographically occult. The incidence of CCM is 0.1%–0.8%[2–4], and individual CCM have reported symptomatic bleeding rates of approximately 1%/year, or 0.25%–3.1%/person/year of exposure[5–7], presenting with headache, seizures, and/or focal neurological deficits. Seizures result from surrounding hemosiderin deposits, cerebral gliosis, and cortical irritation.[8, 9] Supratentorial CCM lead to seizures in up to 70% of patients, and 40% develop medically refractory epilepsy.[10–12] Symptomatic patients may benefit from surgical resection to relieve hemorrhage and mass effect, but to maximize the goal of seizure freedom generally requires more extended lesionectomy of the hemosiderin ring and gliotic tissue.[7, 13–16]

Magnetic resonance thermography (MRT)-guided stereotactic laser ablation (SLA), also referred to as MR-guided laser interstitial thermal therapy (MRgLITT), is a minimally invasive treatment modality for creating precise thermal ablations of pathological tissue such as in brain. Laser energy is delivered via commercially available optical fibers into target tissue where it is converted to thermal energy, inducing cellular injury. The extent of thermal damage relative to structures to be spared is guided by real-time MR-thermography via multi-planar phase mapping[17]. SLA involves heating of tissue to 50–90°C, which causes irreversible parenchymal coagulation and microvascular thrombosis[18, 19], but potentially spares macrovasculature. SLA is an attractive alternative to open surgery and is suitable for a variety of brain pathologies necessitating tissue destruction or disconnection[18–27]. Indeed, we have recently demonstrated that relative to traditional open temporal lobe surgery, SLA

yields superior neurocognitive outcomes[28]. SLA of CCM, however, has not previously been reported.

We reasoned that the angiographically occult nature of CCM implies (1) a low risk of hemorrhage from a stereotactic approach and (2) susceptibility of CCM and surrounding tissue to laser thermal ablation. We report on the feasibility and effectiveness of SLA for cerebral CCM associated with epilepsy in 5 patients with >12 months clinical and imaging outcome.

METHODS

Patient selection

Five successive patients were prospectively enrolled to undergo minimally invasive laser ablation after pre-operative workup for disabling seizures related to the presumed lobar CCM. Each patient's imaging met all classical criteria for CCM including mixed intensity "popcorn" appearance on T2-weighted images, susceptibility artifact indicative of hemosiderin ring on T2*-weighted gradient recalled echo (GRE) and/or T2-weighted images, and lack of surrounding edema on T2-weighted images. Preoperative evaluations typically involved MR imaging, electroencephalography, 18-fluorodeoxyglucose positron emission tomography, and neuropsychometric testing. All patients were offered the alternative of open resection versus SLA, and each patient selected SLA as the initial approach. Informed surgical and research consents (for prospective collection of clinical data as approved by the Emory University Institutional Review Board) were obtained independently, and patients underwent laser ablation between July 2012–January 2014 by either of two surgeons (J.T.W or R.E.G.).

Device for MRT-guided SLA

To perform SLA of CCM, we utilized an FDA-approved, surgical laser ablation system (Visualase® Thermal Therapy System; Medtronic, Inc.) that combines a 15-watt, 980-nm diode laser coupled to an optical fiber with a light-diffusing tip within a light transmitting saline-irrigated cooling sheath[17]. The laser applicator assembly is comprised of an outer 1.6-mm diameter clear (light transmitting) polycarbonate cooling cannula encompassing an inner 0.73-mm diameter flexible laser optical fiber terminating in a 10-mm long diffuser tip. After laser fiber placement by standard stereotactic techniques (described below), treatment was performed in an interventional MRI (iMRI) suite controlled via a stand-alone workstation that is linked via Ethernet connection to the MRI control station. The benefits of using such a system include near real-time thermal monitoring (approximately 4–6 second delay), which allows precise estimation of a zone of irreversible damage (the ablation zone) relative to surrounding structures to be spared (the safety margin). If user-defined undesirable conditions are detected (such as heat spread to the safety margin), the workstation may be set to automatically deactivate the laser as a safety mechanism.[24]

Stereotactic techniques

All procedures were completed under general anesthesia. One of two stereotactic methods of stereotactic laser applicator placement was selected for each patient based upon lesion

location, anticipated approach, and surgeon preference. For subjects 1 and 5 we used a traditional rigid stereotactic head frame (CRW, Integra Neurosciences, Plainsboro, NJ) and the FrameLink® application on the Stealth S7® Workstation (Medtronic®, Louisville, CO) to place a 3.2-mm twist-drill craniostomy-durotomy (via a stab incision) and stereotactic bolt to deliver and secure the laser probe as we have previously described[18]. For subjects 2–4, we used an expendable percutaneously mounted MRI guidance mini-frame and associated guidance software (ScalpMount SmartFrame® and ClearPoint® System, MRI Interventions®, Inc., Memphis, TN) to introduce and secure the probe through a stab incision and 3.2-mm twist-drill craniostomy-durotomy as previously described[18, 19]. Stereotactic planning was performed utilizing volumetric image series (T2 and gadolinium contrasted T1) obtained on a 1.5-Tesla MRI scanner (Magnetom Espree®, Siemens Medical Solutions). Volumetric images were used to plan percutaneous trajectories into the center of CCM that avoided sulci, cerebral veins, and ventricles. In each case, using sterile technique, a single laser applicator was stereotactically introduced to a depth 1–2 cm shallow to the prescribed target depth through a 3.2-mm craniostomy-durotomy. Volumetric imaging confirmed the desired trajectory, the assembly was fully inserted to the prescribed depth within the center of the presumed CCM, and volumetric imaging was again immediately acquired to evaluate final targeting and to evaluate for any evidence of hemorrhage. In all patients in whom this procedure was performed, no evidence of hemorrhage was noted following placement of the laser assembly on MRI.

MRT-guided Laser Treatment

In all cases, we sought to perform extended lesionotomies with ablation zones incorporating both the target CCM and surrounding (presumably epileptogenic) cortex. Two or 3 monitoring planes were selected and specific temperature limits were set for the intended target zone and for surrounding structures, which if exceeded, would automatically trigger cessation of laser energy. Typically, the desired ablation volume was small enough to be included in 1–2 treatment cycles, as the zone of necrosis conformed volumetrically to the structure it was treating. In cases where we sought to extend the length of the ablation volume, the optical fiber was withdrawn in sub-centimeter increments and additional treatment cycles were performed. During the procedure, the workstation presented continuously updated thermal density maps as well as an integrated estimate of damage volume.

Immediate post-treatment MRI was performed obtaining diffusion-weighted imaging (DWI), T2-weighted fluid-attenuated inversion recovery (FLAIR), and gadolinium-enhanced T1-weighted sequences to verify that the lesion and surrounding rim of cortex were thoroughly encompassed in the ablation zone. Laser assemblies were completely removed, stab incisions were closed with absorbable suture, and frames were removed. T2*-weighted GRE sequences were obtained after probe removal to evaluate for acute hemorrhage. Anesthesia was reversed and patients immediately extubated. All patients were admitted for routine ward observation and discharged within 24–36 hours.

Clinical and Imaging Follow-Up

Routine clinical follow-up took place at 6 weeks, 3 months, 6 months, and 12 months in all 5 subjects, and 16–28 months in 4 subjects and included query for any seizures, collection of seizure diaries, review of medications, physical examination, and evaluation of overall clinical status. Patients had follow up MR imaging performed sometime between 6–12 months and additionally at 21 months in one subject to evaluate the structure of the ablated lesion.

Image processing

The acute ablation zone volume on all patients was assessed using a BrainLab workstation (BrainLab AG, Feldkirchen, Germany). Using the pre-treatment T2-weighted MR images, each lesion was traced manually in axial, coronal, and sagittal planes and then rendered volumetrically. The immediate post-treatment contrasted T1-weighted images were used to trace the ablation zone in all three planes and rendered volumetrically. The image sets were co-registered in 3-dimensional space such that pre-treatment lesion volume was overlaid on the ablation volume to estimate the percentage of lesion ablated.

RESULTS

Preoperative features of subjects with epileptogenic CCM

We performed SLA of presumed CCM in 5 successive subjects, ages 28–76 (median 66, mean 54.6) years, with history of epilepsy ranging from 4–52 (median 21, mean 26.4) years (Table 1). In each case, the lesion fulfilled all typical imaging criteria for CCM, as independently reviewed by a board-certified neuroradiologist (AMS) (Figures 1, 2, and 3). Of these lesions, only the one observed in patient 3 (right middle frontal gyrus) appeared somewhat atypical with a more linear/gyriform shape, leaving the possibility of hemorrhagic products from a cause other than CCM. The remaining four lesions were temporal, of which one was mesial temporal (right hippocampus, patient 2), and three were inferolateral temporal (left fusiform gyrus in patient 1, left fusiform and inferior temporal gyri in patient 4, and left inferior temporal gyrus in patient 5). Subject 5 also exhibited a developmental venous anomaly contiguous to the presumed CCM. The location of each lesion on MRI was concordant with localization of hypometabolism on PET co-registered imaging and with localization of apparent seizure onset by noninvasive video electroencephalographic (EEG) studies, with the exception of subject 4 in whom PET imaging was not performed. Specific preoperative neuropsychological findings were largely consistent with localization of presumed epileptic foci in each subject. All subjects had evidence of strongly or modestly concordant cognitive deficits (consistent with expected laterality and lobar localization), although two patients (subjects 1 and 2) had at least some neuropsychometric evidence of additional deficits (Table 1).

Imaging results of laser ablation

Relevant imaging of stereotactic laser fiber placement, treatment, and ablation results are shown for subject 1 (Figure 1), subjects 2–4 (Figure 2), and subject 5 (Figure 3). Via transtemporal, transoccipital, or transfrontal approaches, laser fiber applicators were placed

accurately into presumed CCM in all subjects without complication. Specifically, we observed no evidence of acute hemorrhage immediately following insertion to target depth in any subject. In each case we performed near real-time thermal therapy with the goal of ablating a tissue volume encompassing the CCM and surrounding parenchyma.

Notably, due to the effects upon T2*-GRE images of concentrated blood products within CCM, we observed small areas of thermal signal dropout, which yielded some lack of confluence in thermal imaging within the boundaries of each CCM (evident in Figure panels 1E, 1F, 2C, 2H, 2M, 3C, and 3D). However, thermal imaging was not limited in the cortex surrounding each CCM, corresponding to areas of presumed epileptogenicity, and these were incorporated within desired ablation zones without technical difficulty. Thus, despite technical limitations of monitoring temperature in a confluent manner within CCM, thermal imaging provided sufficient evidence of ablation to easily guide extended lesionotomy in each case. Indeed, desired extent of ablation was verified by immediate post-ablation T2-FLAIR, DWI, and post-contrast T1-weighted sequences in each case.

In the particular case of subject 5, the CCM was in direct apposition to the lateral temporal vein of Labbé (Figure 3). Thermal imaging during delivery of laser therapy demonstrated heating of the CCM and brain parenchyma while focally sparing the immediate vicinity of the vein (Figure 3C, D), likely due to expected thermal energy sink caused by continuing flow through the vein, but also possibly due to signal dropout as described above. Immediate post-ablation anatomical imaging verified that a wide ablation of the lesion and surrounding cortex was safely performed, as there was no evidence of collateral vascular injury (Figure 3E, G), and diffusion restriction was isolated to the intended ablation zone (Figure 3H).

Postoperative analysis revealed that estimated acute ablation volumes (from post-contrast T1-weighted images) were more extensive than estimated preoperative CCM volumes (from T2-weighted images) in each case (Table 2). However, direct volume overlays demonstrated that postoperative ablation zones encompassed 80%–98% (mean 91.4%) of individual CCM volumes, resulting either from technical limitations in image processing and alignment and/or residual lesion tissue in each case. Notably for subject 5, volumetric modeling of the contiguous vein of Labbé revealed no immediate postprocedural changes in vein morphology or diameter despite surrounding evidence of parenchymal ablation (Figure 3I, J).

Repeat MRI at 6–21 months post-ablation was obtained for comparison to preoperative imaging in all subjects. In subject 1 at 6 months post-ablation, the CCM was slightly smaller on T2-weighted fast spin echo and T2*-GRE images, and there was more T2 hypointensity centrally within the ablated CCM, corresponding to blood products (methemoglobin) (Figure 1H, I). Pre-contrast T1-weighted images at 6 months demonstrated increased areas of hyperintensity within the center of the CCM (also consistent with blood products), and post-contrast T1-weighted images showed faint increased enhancement within the center of the ablated CCM (not shown). Around the CCM itself there was interval development of a surrounding volume of marked T1 hypointensity, which corresponded to extremely high T2 signal (Figure 1H), compatible with fluid signal intensity from liquefaction. Repeat imaging

of subject 1 again at 21 months revealed obvious evolving diminution of the lesion within a stable area of encephalomalacia (Figure 1J).

Post-ablation imaging of subject 2 at 12 months (Figure 2E), subject 3 at 6 months (Figure 2J), and subject 4 at 11 months (Figure 2O) likewise revealed corresponding regions of parenchymal T1 hypointensity and T2 hyperintensity (encephalomalacia) and central focal hypointensity (methemoglobin) at the location of prior CCM. Post-ablation imaging of subject 5 at 6 months similarly revealed a T2 iso- to hypointense tissue, markedly reduced in the size, and surrounded by parenchymal T1 hypointensity and T2 hyperintensity from liquefaction (Figure 3L). Again noted was complete preservation of the contiguous vein of Labbé.

Overall, the findings of post-ablation interval imaging suggest that thermal laser ablation resulted in shrinkage of CCM, and left a zone of necrotic encephalomalacia around the targeted CCM, consistent with the procedural goal of generating an extended lesionotomy. Further diminution and resolution of methemoglobin and hemosiderin with time was demonstrated by serial imaging in subject 1. No evidence of delayed or widespread hemorrhagic complications of the procedure was apparent in any subjects.

Clinical outcomes

Following the surgical procedures, no adverse events or gross neurological deficits were encountered, and all patients were discharged on postoperative day 1 or 2 (<36 h). There were no emergency department visits or readmissions of any patient during the follow-up period. No patients reported significant or new headaches during the follow-up period. No new focal or global neurological deficits were noted in any of the patients.

With respect to epilepsy outcomes following SLA alone, 4 of 5 patients were free of seizures impairing awareness (Engel class 1) at 12–28 (median 16, mean 17.4) months (Table 2). Of these, patient 1 was Engel 1A (completely free of seizures), patient 2 was Engel 1B (auras on a single day after a medication reduction), patient 4 was Engel 1D (the patient discontinued all medications against medical advice and subsequently had a single generalized tonic seizure during an episode of binge drinking alcohol), and patient 5 was Engel 1B (two brief episodes of presumed simple partial seizure in which she had difficulty speaking without impaired awareness after a medication reduction). Patient 3, who showed no appreciable change at 6 months following SLA (Engel class 4B), exhibited MRI evidence of focal atrophy without persistent blood products at the ablation site (Figure 2J). She subsequently underwent intracranial grid placement for seizure localization. This resulted in more extensive resection of the middle frontal gyrus (including the area of prior ablation). Consistent with imaging, we found no gross evidence of tissue resembling CCM intraoperatively. Final pathological diagnosis of specimens sent from the epileptogenic zone was described as cortical parenchyma with reactive gliosis. Postoperative imaging confirmed a resection area incorporating, but much wider than the area of previously presumed CCM and ablation. She remained seizure-free at 12 months following open resection.

DISCUSSION

Recent studies have demonstrated the safe and effective use of minimally invasive MRT-guided SLA on multiple intracranial lesion types using one of two commercially available MRgLITT systems. Previously reported applications have included mesial temporal epilepsy[18], insular epilepsy[21, 29], hypothalamic hamartomas[30], metastases[31, 32], gliomas[29, 33–35], periventricular nodular heterotopias[36], and symptomatic radiation necrosis[25]. To our knowledge, however, SLA of CCM has not been previously attempted, possibly due to potential risk of hemorrhage from stereotactic device insertion into these vascular lesions. However, the angiographically occult nature of CCM, portending a low flow state, argues that such risk may be acceptable. Indeed, we found that our novel SLA approach precisely accomplished the goal of minimally invasive extended lesionotomy and was safe in that no complications (i.e. hemorrhages) were evident in this small series. We detected no gross neurologic deficits; the neuropsychometric results of focal temporal lobe ablations will be the subject of a larger independent study by our group.

Operative management of CCM is indicated for highly symptomatic lesions, such as those presenting with drug-resistant epilepsy. Open microsurgical resection of the CCM and its hemosiderin rim, which is associated with seizure control in approximately 75% of patients, is considered optimal treatment for CCM-related epilepsy[37]. Stereotactic radiosurgery is a minimally invasive alternative for CCM, but produces delayed and variable rates of seizure freedom (25%–64% of patients)[38–40]. In a larger study of 49 radiosurgery patients, 53% were seizure-free[38], but patients with simple partial seizures responded better than those with the most disabling complex partial seizures. All subjects in our study fell into this more disabling category.

Both gold standard open microsurgery and its current alternative, radiosurgery, carry risks of complications. On one hand, microsurgery is less favorable where it risks collateral injury to deep or eloquent regions. On the other, radiotherapy risks higher rates of recurrent hemorrhage and symptomatic edema from radiation necrosis.[41–44] By comparison, SLA in our series compares favorably to these standard techniques: SLA produced immediate therapeutic effects without evidence of collateral damage from approach, hemorrhage, or clinical side effects relatable to edema. Seizure control in our small series was similar to that generally expected for open microsurgery. However, because epileptogenic networks could vary unpredictably by lesion, local anatomy, and other patient-specific factors, it seems unlikely that SLA alone could provide persistent rates of seizure freedom superior to intracranial electrode-guided resections in all cases. Indeed, one of 5 patients in our series had no benefit from SLA, but achieved seizure freedom only after intracranial monitoring and resection. Indeed, this option was initially provided, but given her age (67 y) and preference for the minimally invasive approach, laser ablation was attempted first. Notably, this is also the only subject in the series with atypical imaging features (Table 1), potentially challenging whether the ablated lesion was a CCM.

On balance, SLA is a novel and attractive option with preliminary evidence of efficacy against seizures and a potentially acceptable risk profile. Full evaluation of SLA compared

to other approaches with respect to safety, seizure control, and neurocognitive risk will require additional studies and longer follow-up.

Beyond epilepsy, interventions for cerebral or deep brain cavernous malformations may be indicated for recurrent symptomatic hemorrhage and/or mass effect. Recurrent hemorrhage can be devastating in basal ganglia, thalamus, and brainstem, necessitating surgery despite the risks of microsurgical access or symptomatic radiation necrosis in deep brain structures. While we observed no hemorrhagic complications with our stereotactic approach to epileptic lobar CCM, the safety and efficacy of this approach to hemorrhagic and/or deep brain cavernous malformations is unknown. Furthermore, our observation that intrinsic signal characteristics of CCM can confound confluent thermal imaging within the malformation itself, increasing reliance upon thermal changes in surrounding parenchyma could prove challenging in cases where injury to surrounding brain parenchyma would be intolerable (e.g. brainstem cavernous malformation). Only ablation of a variety of lesions and longer-term follow-up will determine whether SLA would prevent recurrent hemorrhage or progression of cavernous malformations of various locations.

CONCLUSION

MRT-guided SLA is a minimally invasive alternative to open surgery with the potential to minimize collateral injury to off-target structures. Our early experience with SLA of 5 presumed CCM demonstrates this approach to be safe, feasible, and well tolerated. SLA holds promise as a first-line therapy for surgical management of cerebral CCM.

Acknowledgments

FINANCIAL SUPPORT and INDUSTRY AFFILIATIONS: Funding was provided to Emory University by way of a clinical study agreement from Visualase, Inc., which developed products related to the research described in this paper. In addition, REG served as a consultant to Visualase, Inc. and Medtronic, Inc. and received compensation for these services. BF is a former employee and stockholder in Visualase, Inc. DLD receives funding from the NIH/NINDS (K02 NS070960), which provides support for his work. JTW is a consultant for Medtronic, Inc. and MRI Interventions, Inc.

We thank Emilee Holland and Gregory Johnstone for clinical research coordination.

References

1. Raychaudhuri R, Batjer HH, Awad IA. Intracranial cavernous angioma: a practical review of clinical and biological aspects. Surgical neurology. 2005 Apr; 63(4):319–328. discussion 328. [PubMed: 15808709]
2. Baumann CR, Schuknecht B, Lo Russo G, et al. Seizure outcome after resection of cavernous malformations is better when surrounding hemosiderin-stained brain also is removed. Epilepsia. 2006 Mar; 47(3):563–566. [PubMed: 16529622]
3. Brelie, Cvd; von Lehe, M.; Raabe, A., et al. Surgical Resection Can Be Successful in a Large Fraction of Patients With Drug-Resistant Epilepsy Associated With Multiple Cerebral Cavernous Malformations. Neurosurgery. 2014; 74(2):147–153. [PubMed: 24435138]
4. Kim W, Stramotas S, Choy W, Dye J, Nagasawa D, Yang I. Prognostic factors for post-operative seizure outcomes after cavernous malformation treatment. Journal of clinical neuroscience : official journal of the Neurosurgical Society of Australasia. 2011 Jul; 18(7):877–880. [PubMed: 21561775]
5. Kim M, Rowed DW, Cheung G, Ang LC. Cavernous malformation presenting as an extra-axial cerebellopontine angle mass: case report. Neurosurgery. 1997 Jan; 40(1):187–190. [PubMed: 8971841]

6. Stefan H, Hammen T. Cavernous haemangiomas, epilepsy and treatment strategies. Acta neurologica Scandinavica. 2004 Dec; 110(6):393–397. [PubMed: 15527452]
7. Ferroli P, Casazza M, Marras C, Mendola C, Franzini A, Broggi G. Cerebral cavernomas and seizures: a retrospective study on 163 patients who underwent pure lesionectomy. Neurological sciences : official journal of the Italian Neurological Society and of the Italian Society of Clinical Neurophysiology. 2006 Feb; 26(6):390–394.
8. Steiger HJ, Markwalder TM, Reulen HJ. Clinicopathological relations of cerebral cavernous angiomas: observations in eleven cases. Neurosurgery. 1987 Dec; 21(6):879–884. [PubMed: 3325850]
9. Awad I, Jabbour P. Cerebral cavernous malformations and epilepsy. Neurosurgical focus. 2006; 21(1):e7. [PubMed: 16859260]
10. Chang EF, Gabriel RA, Potts MB, Berger MS, Lawton MT. Supratentorial cavernous malformations in eloquent and deep locations: surgical approaches and outcomes. Clinical article. Journal of neurosurgery. 2011 Mar; 114(3):814–827. [PubMed: 20597603]
11. Moran NF, Fish DR, Kitchen N, Shorvon S, Kendall BE, Stevens JM. Supratentorial cavernous haemangiomas and epilepsy: a review of the literature and case series. Journal of neurology, neurosurgery, and psychiatry. 1999 May; 66(5):561–568.
12. Ryvlin P, Mauguiere F, Sindou M, Froment JC, Cinotti L. Interictal cerebral metabolism and epilepsy in cavernous angiomas. Brain : a journal of neurology. 1995 Jun; 118(Pt 3):677–687. [PubMed: 7600085]
13. Yeon JY, Kim JS, Choi SJ, Seo DW, Hong SB, Hong SC. Supratentorial cavernous angiomas presenting with seizures: surgical outcomes in 60 consecutive patients. Seizure : the journal of the British Epilepsy Association. 2009 Jan; 18(1):14–20.
14. Alonso-Vanegas MA, Cisneros-Franco JM, Otsuki T. Surgical management of cavernous malformations presenting with drug-resistant epilepsy. Frontiers in neurology. 2011; 2:86. [PubMed: 22319505]
15. Komotar RJ, Mikell CB, McKhann GM 2nd. "Epilepsy surgery" versus lesionectomy in patients with seizures secondary to cavernous malformations. Clinical neurosurgery. 2008; 55:101–107. [PubMed: 19248674]
16. Wang X, Tao Z, You C, Li Q, Liu Y. Extended resection of hemosiderin fringe is better for seizure outcome: a study in patients with cavernous malformation associated with refractory epilepsy. Neurology India. 2013 May-Jun;61(3):288–292. [PubMed: 23860150]
17. McNichols RJ, Gowda A, Kangasniemi M, Bankson JA, Price RE, Hazle JD. MR thermometry-based feedback control of laser interstitial thermal therapy at 980 nm. Lasers in surgery and medicine. 2004; 34(1):48–55. [PubMed: 14755424]
18. Willie JT, Laxpati NG, Drane DL, et al. Real-Time Magnetic Resonance-Guided Stereotactic Laser Amygdalohippocampotomy for Mesial Temporal Lobe Epilepsy. Neurosurgery. 2014 Mar 10.
19. Willie JTGR, Mehta A, Sharon A, Sperling MR, Curry DJ, Wilfong A, Marsh WR, Danish SF, Wong S, Weinhand M, Langevin JP, Labiner D, Couture D, Tandon N, Kalamangalam G. Multicenter Experience with Minimally Invasive Stereotactic Laser Thermal Amygdalohippocampectomy for Mesial Temporal Lobe Epilepsy. Epilepsia. 2013; 54(Suppl. 3): 290.
20. Carpentier A, McNichols RJ, Stafford RJ, et al. Laser thermal therapy: real-time MRI-guided and computer-controlled procedures for metastatic brain tumors. Lasers in surgery and medicine. 2011 Dec; 43(10):943–950. [PubMed: 22109661]
21. Curry DJ, Gowda A, McNichols RJ, Wilfong AA. MR-guided stereotactic laser ablation of epileptogenic foci in children. Epilepsy & behavior : E&B. 2012 Aug; 24(4):408–414.
22. Schwarzmaier HJ, Eickmeyer F, von Tempelhoff W, et al. MR-guided laser-induced interstitial thermotherapy of recurrent glioblastoma multiforme: preliminary results in 16 patients. European journal of radiology. 2006 Aug; 59(2):208–215. [PubMed: 16854549]
23. Schwarzmaier HJ, Eickmeyer F, von Tempelhoff W, et al. MR-guided laser irradiation of recurrent glioblastomas. Journal of magnetic resonance imaging : JMRI. 2005 Dec; 22(6):799–803. [PubMed: 16270287]

24. Tovar-Spinoza Z, Carter D, Ferrone D, Eksioglu Y, Huckins S. The use of MRI-guided laser-induced thermal ablation for epilepsy. Child's nervous system : ChNS : official journal of the International Society for Pediatric Neurosurgery. 2013 Jun 4.
25. Rao MS, Hargreaves EL, Khan AJ, Haffty BG, Danish SF. Magnetic Resonance-Guided Laser Ablation Improves Local Control for Post-Radiosurgery Recurrence and/or Radiation Necrosis. Neurosurgery. 2014 Feb 27.
26. Carpentier A, Chauvet D, Reina V, et al. MR-guided laser-induced thermal therapy (LITT) for recurrent glioblastomas. Lasers in surgery and medicine. 2012 Jul; 44(5):361–368. [PubMed: 22488658]
27. Carpentier A, McNichols RJ, Stafford RJ, et al. Real-time magnetic resonance-guided laser thermal therapy for focal metastatic brain tumors. Neurosurgery. 2008 Jul; 63(1 Suppl 1):ONS21–ONS28. discussion ONS28–29. [PubMed: 18728600]
28. Drane DL, Loring DW, Voets NL, Price M, Gross RE, Willie JT, Helmers SL, Ojemann JG, Phatak V, Miller JW, Meador KW. Temporal Lobe Epilepsy Surgical Patients Undergoing MRI-guided Stereotactic Laser Ablation Exhibit Better Episodic Memory Outcome as Compared to Standard Surgical Approaches. Epilepsia. 2013; 54(Suppl. 3):20. [PubMed: 24001064]
29. Hawasli AH, Bagade S, Shimony JS, Miller-Thomas M, Leuthardt EC. Magnetic resonance imaging-guided focused laser interstitial thermal therapy for intracranial lesions: single-institution series. Neurosurgery. 2013 Dec; 73(6):1007–1017. [PubMed: 24056317]
30. Wilfong AA, Curry DJ. Hypothalamic hamartomas: optimal approach to clinical evaluation and diagnosis. Epilepsia. 2013 Dec; 54(Suppl 9):109–114. [PubMed: 24328883]
31. Jethwa PR, Barrese JC, Gowda A, Shetty A, Danish SF. Magnetic resonance thermometry-guided laser-induced thermal therapy for intracranial neoplasms: initial experience. Neurosurgery. 2012 Sep; 71(1 Suppl Operative):133–144. 144–135. [PubMed: 22653396]
32. Hawasli AH, Ray WZ, Murphy RK, Dacey RG Jr, Leuthardt EC. Magnetic resonance imaging-guided focused laser interstitial thermal therapy for subinsular metastatic adenocarcinoma: technical case report. Neurosurgery. 2012 Jun; 70(2 Suppl Operative):332–337. discussion 338. [PubMed: 21869722]
33. Jethwa PR, Lee JH, Assina R, Keller IA, Danish SF. Treatment of a supratentorial primitive neuroectodermal tumor using magnetic resonance-guided laser-induced thermal therapy. Journal of neurosurgery. Pediatrics. 2011 Nov; 8(5):468–475. [PubMed: 22044371]
34. Sloan AE, Ahluwalia MS, Valerio-Pascua J, et al. Results of the NeuroBlate System first-in-humans Phase I clinical trial for recurrent glioblastoma: clinical article. Journal of neurosurgery. 2013 Jun; 118(6):1202–1219. [PubMed: 23560574]
35. Leonardi MA, Lumenta CB. Stereotactic guided laser-induced interstitial thermotherapy (SLITT) in gliomas with intraoperative morphologic monitoring in an open MR: clinical expierence. Minimally invasive neurosurgery : MIN. 2002 Dec; 45(4):201–207. [PubMed: 12494354]
36. Esquenazi Y, Kalamangalam GP, Slater JD, et al. Stereotactic laser ablation of epileptogenic periventricular nodular heterotopia. Epilepsy research. 2014 Mar; 108(3):547–554. [PubMed: 24518890]
37. Rosenow F, Alonso-Vanegas MA, Baumgartner C, et al. Cavernoma-related epilepsy: review and recommendations for management--report of the Surgical Task Force of the ILAE Commission on Therapeutic Strategies. Epilepsia. 2013 Dec; 54(12):2025–2035. [PubMed: 24134485]
38. Bartolomei F, Regis J, Kida Y, et al. Gamma Knife radiosurgery for epilepsy associated with cavernous hemangiomas: a retrospective study of 49 cases. Stereotactic and functional neurosurgery. 1999; 72(Suppl 1):22–28. [PubMed: 10681687]
39. Sakamoto S, Ohba S, Eguchi K, et al. Churg-Strauss syndrome presenting with subarachnoid hemorrhage from ruptured dissecting aneurysm of the intracranial vertebral artery. Clinical neurology and neurosurgery. 2005 Aug; 107(5):428–431. [PubMed: 16023541]
40. Hsu PW, Chang CN, Tseng CK, et al. Treatment of epileptogenic cavernomas: surgery versus radiosurgery. Cerebrovascular diseases. 2007; 24(1):116–120. discussion 121. [PubMed: 17536202]
41. Kondziolka D, Flickinger JC, Lunsford LD. Stereotactic radiosurgery for epilepsy and functional disorders. Neurosurgery clinics of North America. 2013 Oct; 24(4):623–632. [PubMed: 24093580]

42. Hensley-Judge H, Quigg M, Barbaro NM, et al. Visual field defects after radiosurgery for mesial temporal lobe epilepsy. Epilepsia. 2013 Aug; 54(8):1376–1380. [PubMed: 23663063]

43. Kondziolka D. Epilepsy and radiosurgery. Journal of neurosurgery. 2012 Jun.116(6):1219. discussion 1220. [PubMed: 22443501]

44. Barbaro NM, Quigg M, Broshek DK, et al. A multicenter, prospective pilot study of gamma knife radiosurgery for mesial temporal lobe epilepsy: seizure response, adverse events, and verbal memory. Annals of neurology. 2009 Feb; 65(2):167–175. [PubMed: 19243009]

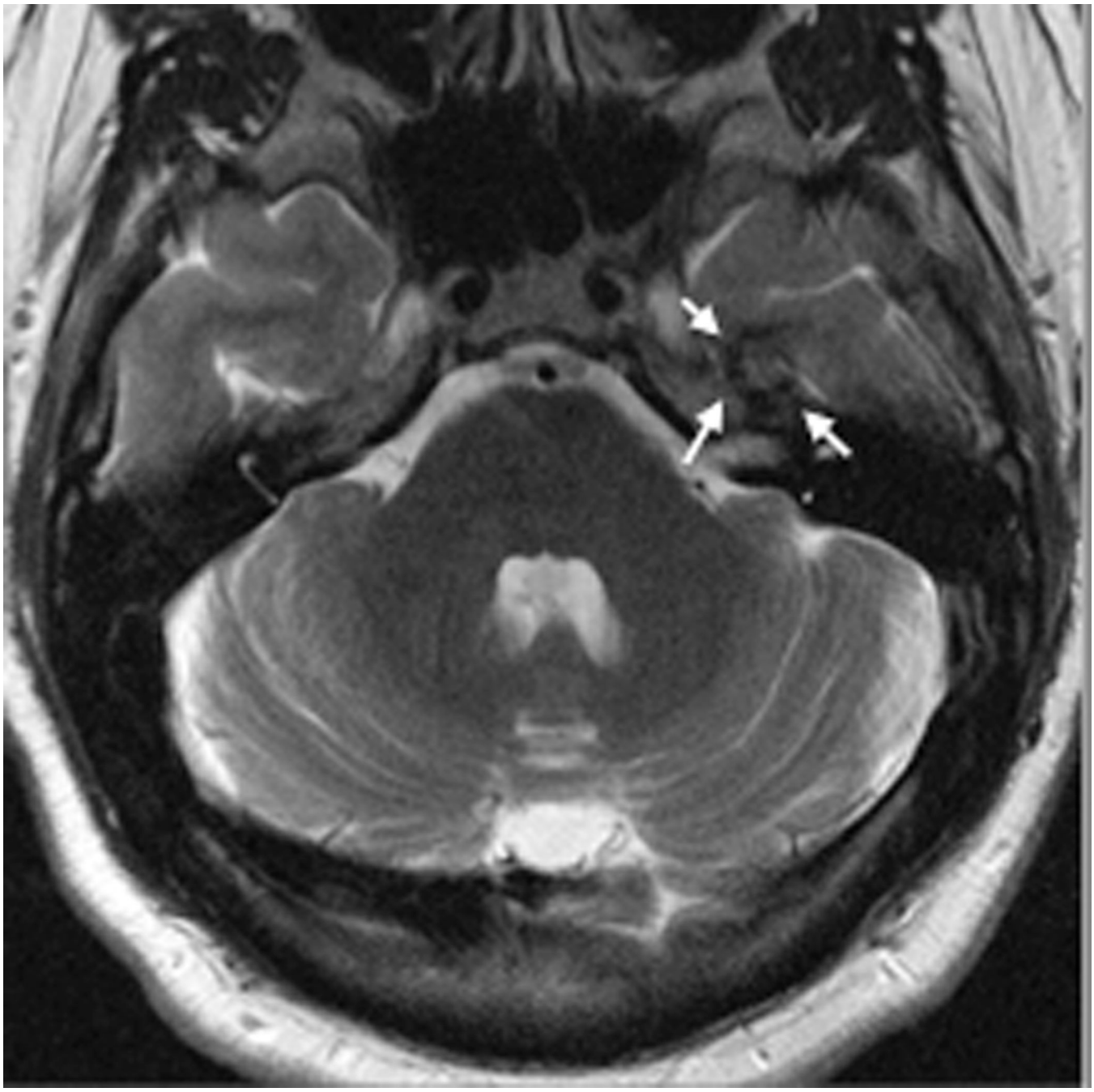

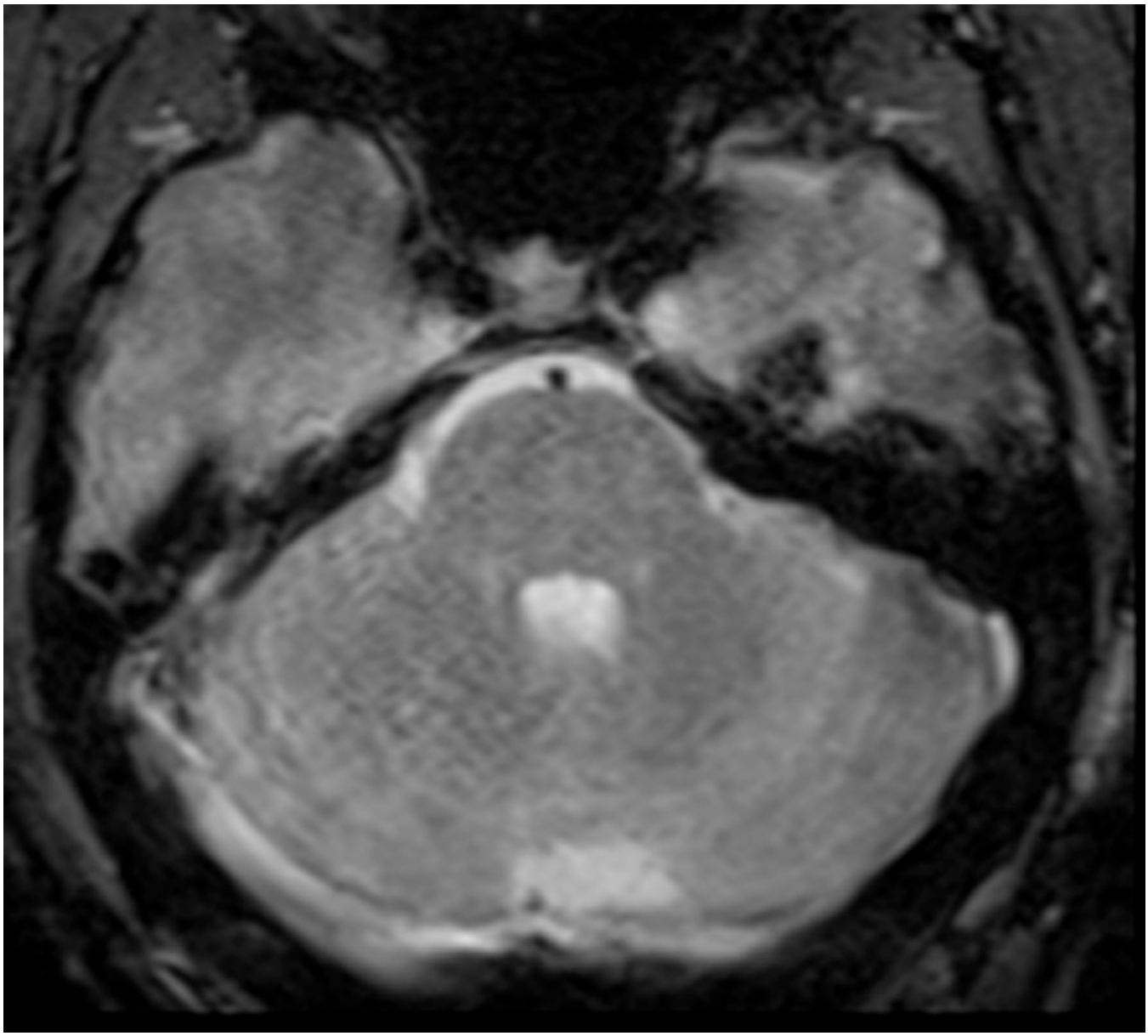

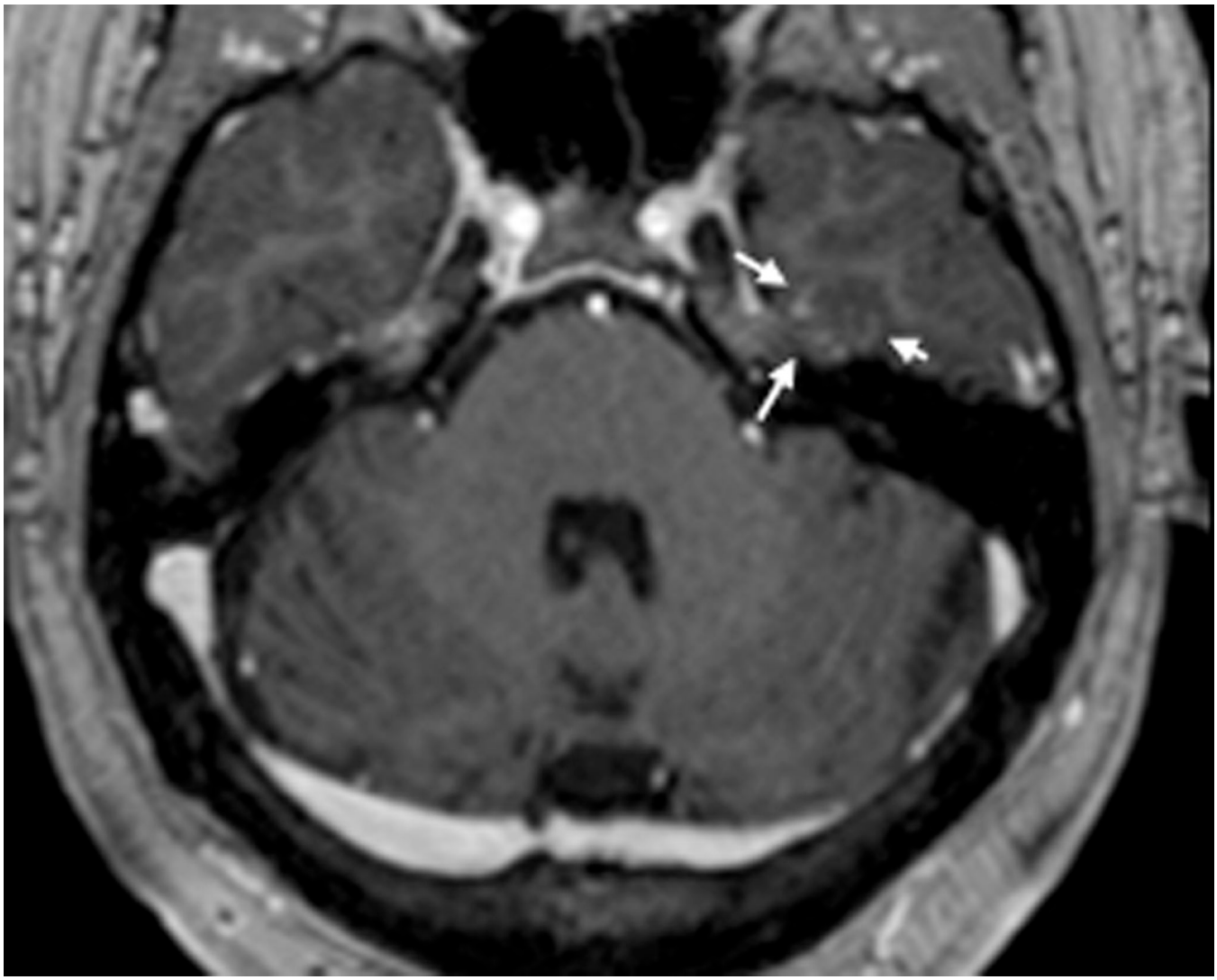

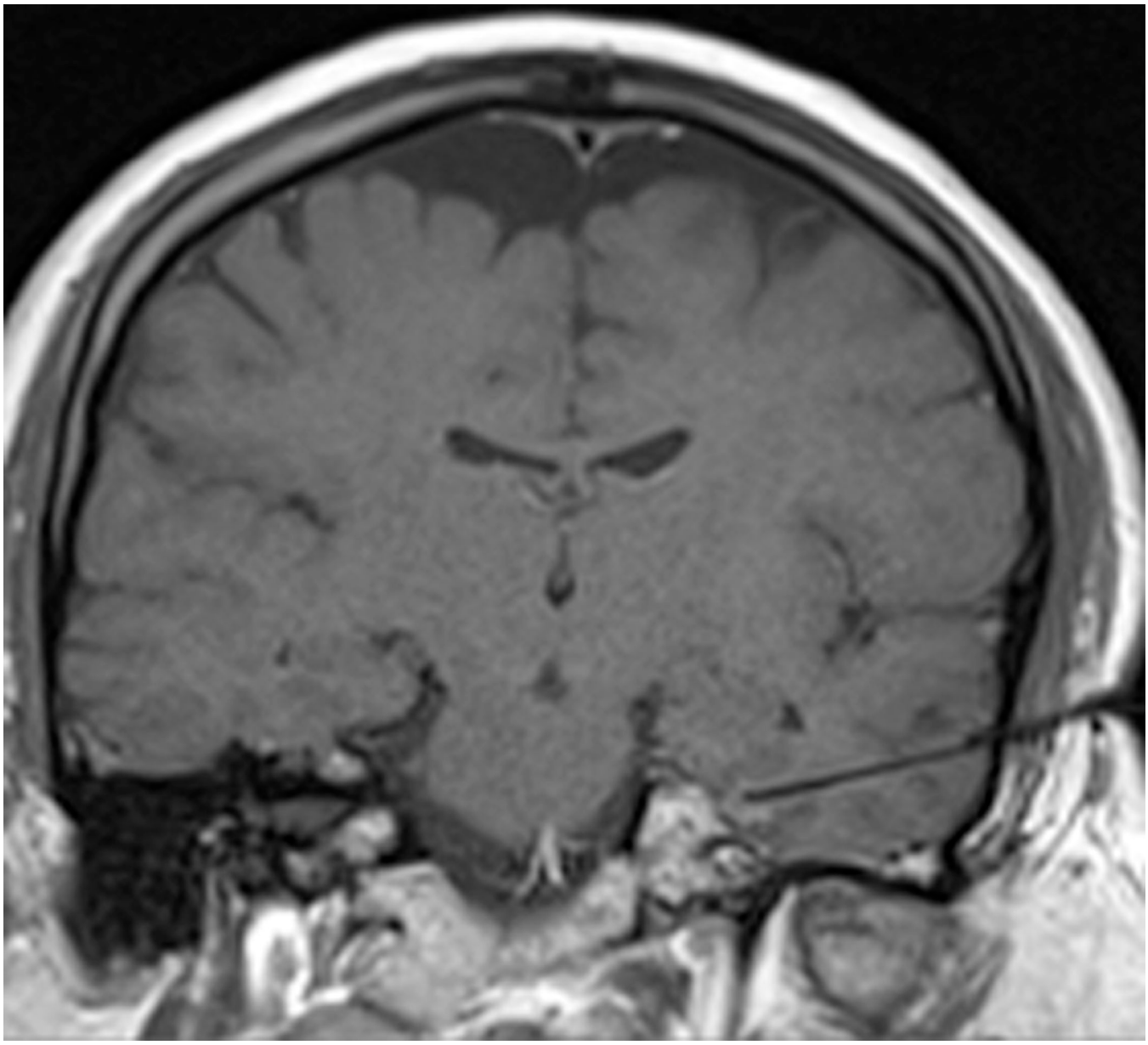

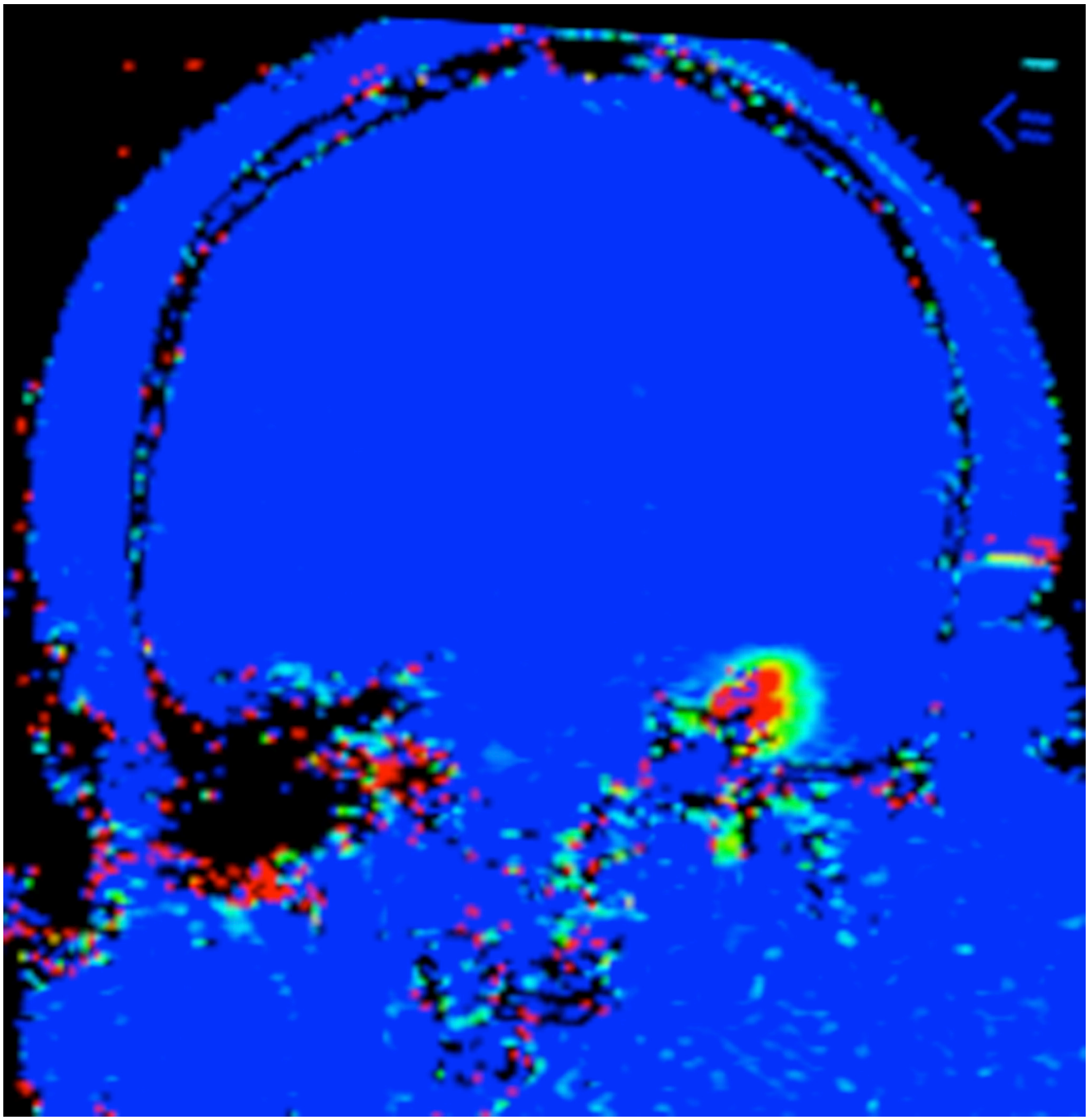

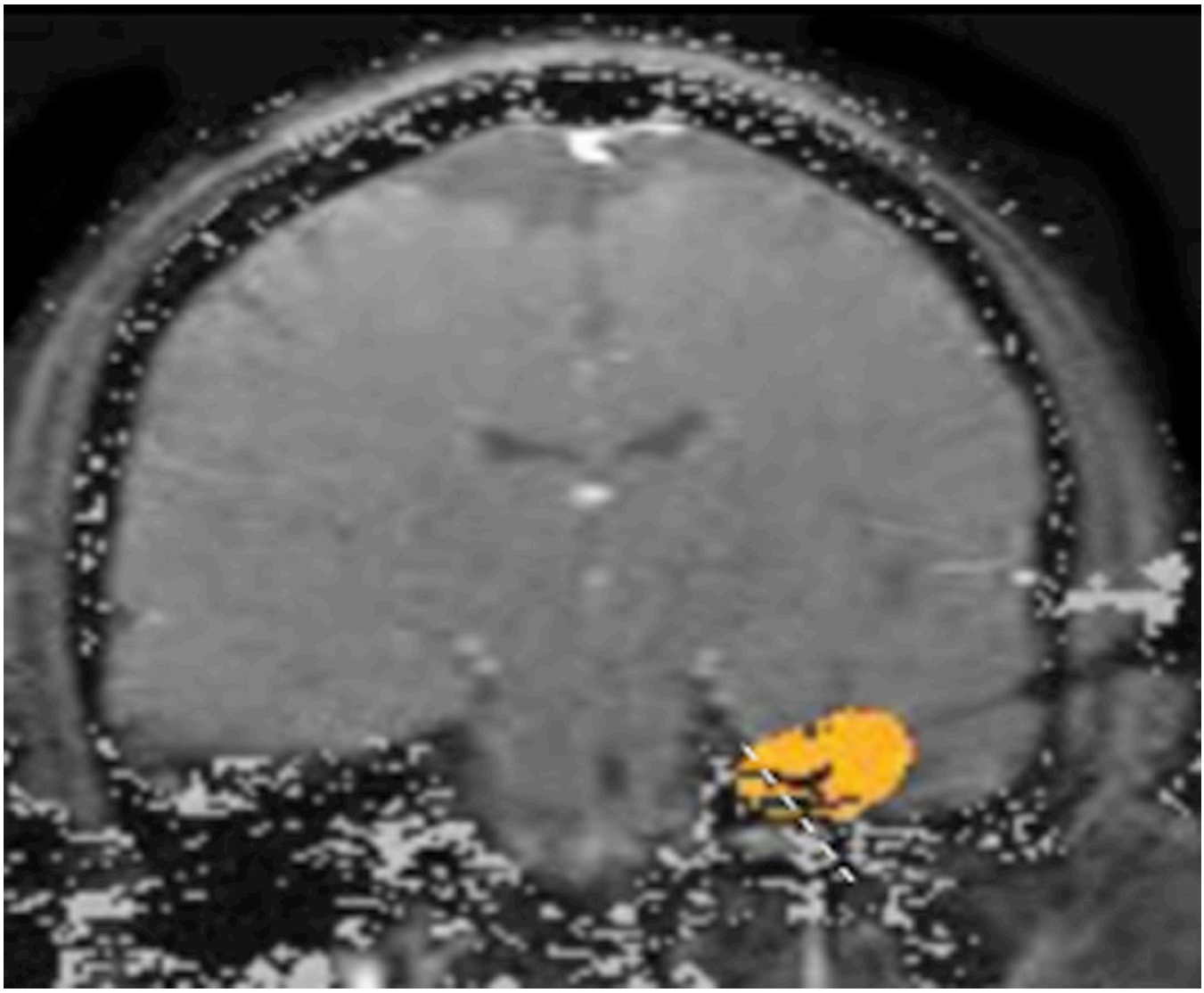

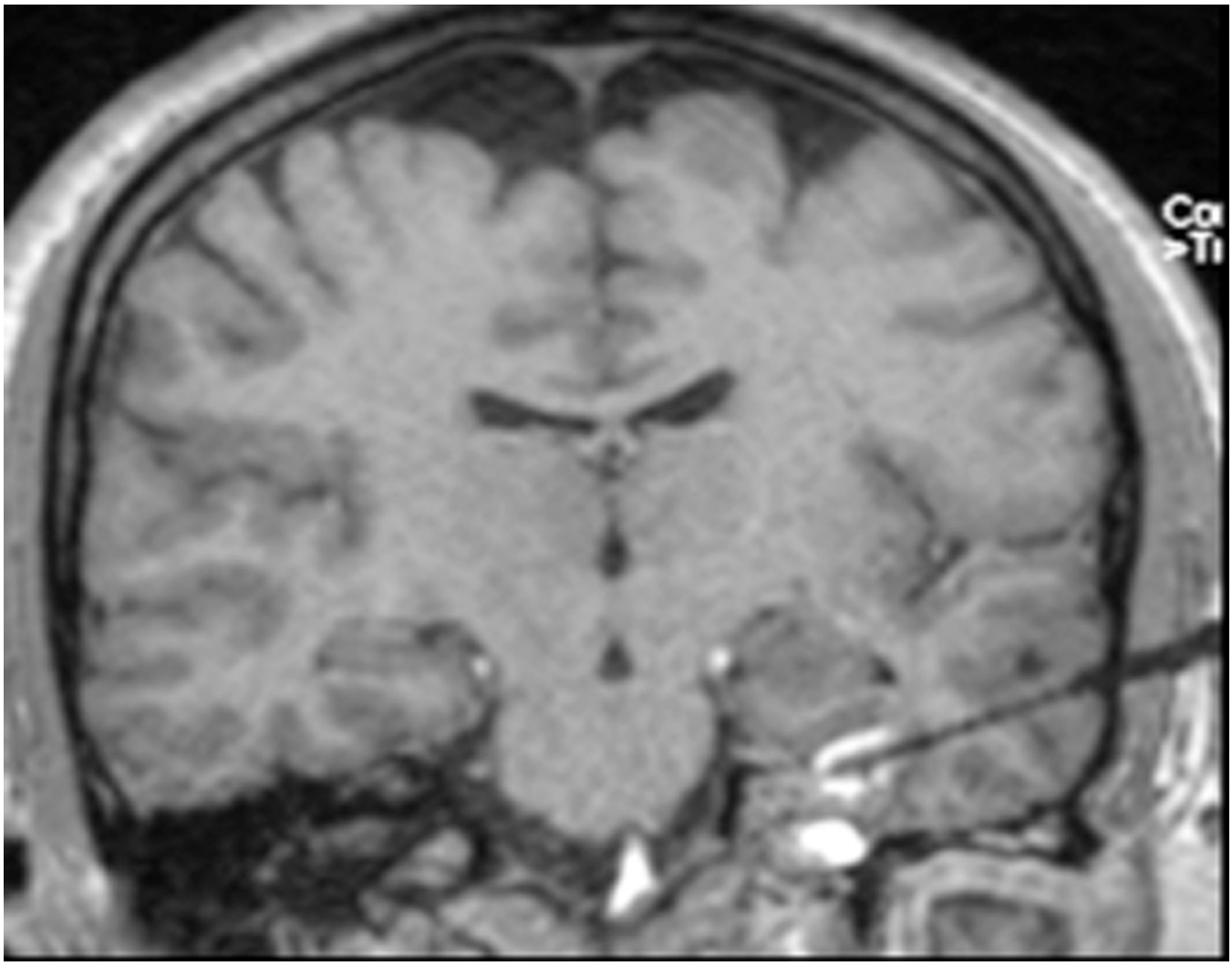

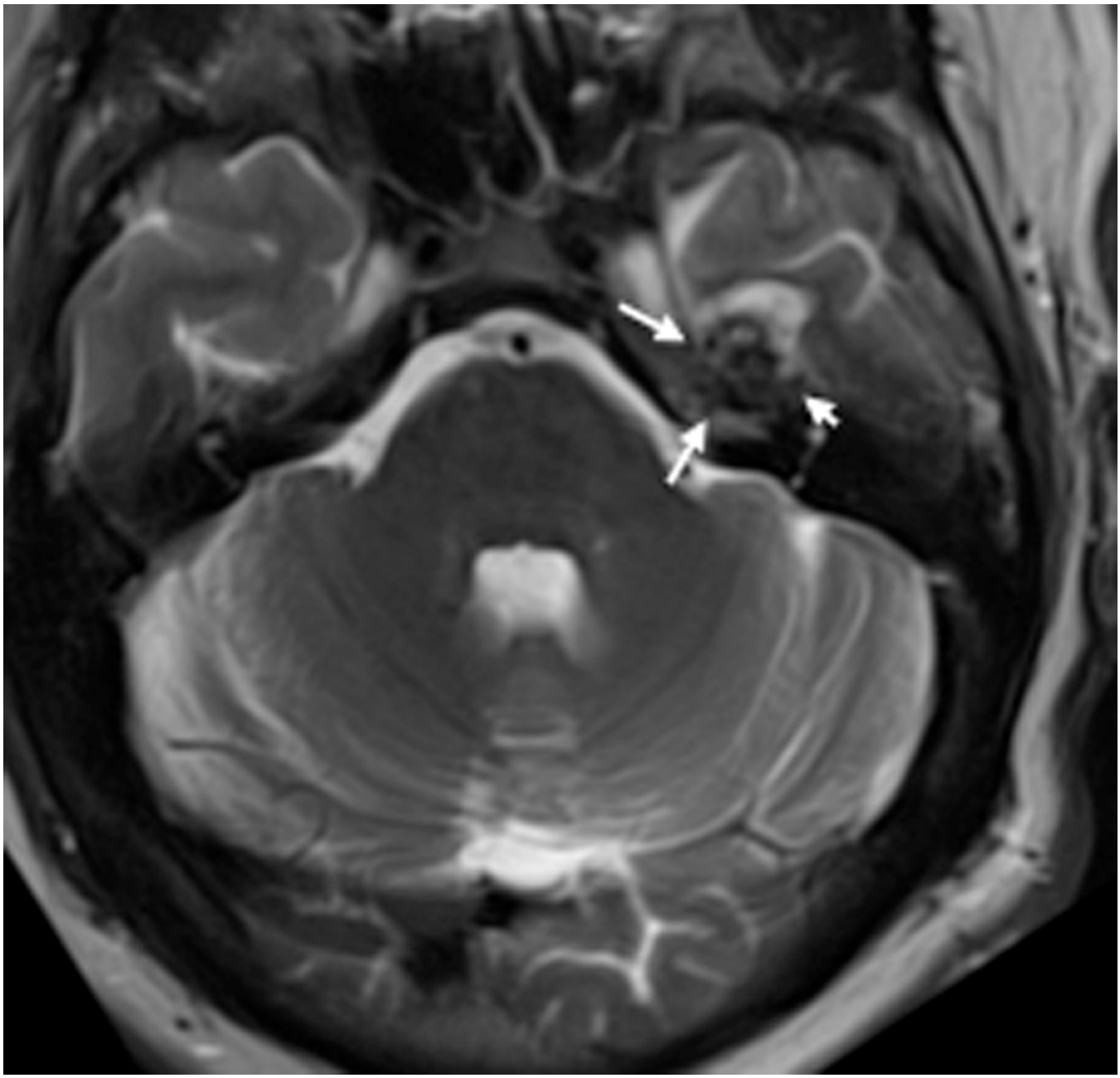

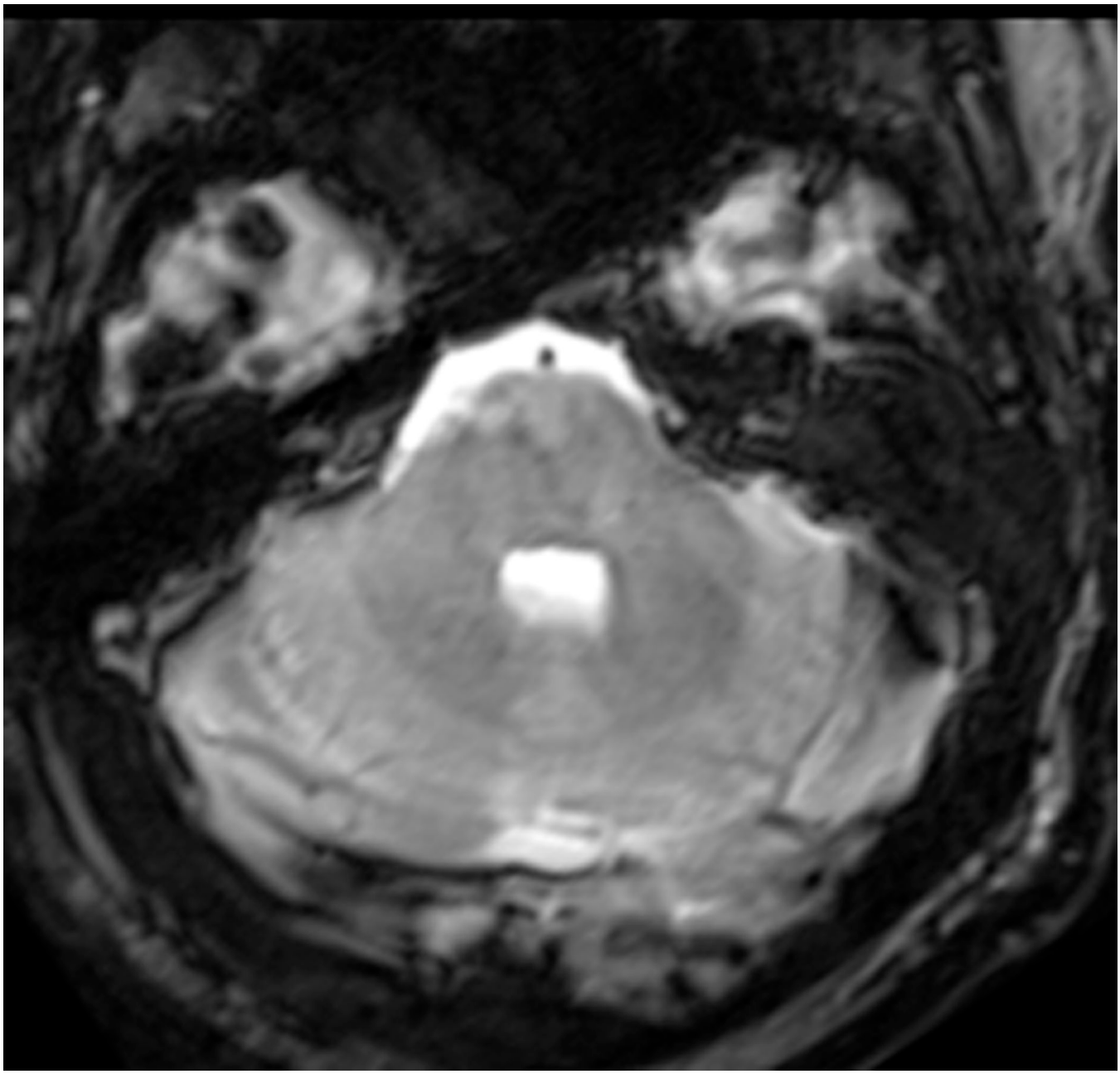

FIGURE 1. Magnetic resonance thermometry-guided stereotactic laser thermal ablation of a putative cerebral cavernous malformation (CCM) associated with epilepsy in subject 1

Preoperative axial T2-weighted fast spin echo (**A**), T2*-weighted gradient recalled echo (GRE) (**B**), and gadolinium-enhanced T1-weighted (**C**) MR images demonstrate a lesion consistent with CCM (arrows) in the superficial fusiform gyrus near the skull base. Intraoperative coronal MR images (**D–G**): **D**, T1-weighted image demonstrates stereotactic placement of cannula and optical fiber into the CCM without evidence of acute hemorrhage or mass effect. Dotted white line delineates margin of skull base for reference. **E**, Thermal

imaging (blue 37–46°C, green 57–66°C, yellow 67–76°C, red >76°C) as shown on the laser workstation during laser interstitial thermal therapy. Note small areas of signal dropout (blue contiguous with red) within the ablation core, presumably due to proximity to the skull base or the effects of intrinsic blood products associated with CCM upon GRE-based thermal imaging. **F**, Estimate of the total zone of irreversible laser ablation as shown on the laser workstation during therapy. **G**, Immediate post-procedure coronal post-contrast T1-weighted image demonstrating increased enhancement (ablation zone) at the location of the CCM. Repeat axial imaging obtained at 6 months post-procedure exemplified by T2-weighted (**H**) and T2*-GRE (**I**) images demonstrate changes in the CCM and surrounding cortex relative to corresponding preoperative images (**A** and **B**, respectively). At 6 months, the CCM appeared slightly smaller on T2 and GRE images, and there was more T2 hypointensity centrally within the ablated CCM, corresponding to blood products (methemoglobin). Post-contrast T1-weighted images (not shown) showed slightly increased enhancement within the center of the ablated CCM. Around the region of the CCM itself there had been interval development of a surrounding area of marked T1 hypointensity, which corresponded to extremely high T2 signal (**H**), compatible with fluid signal intensity from liquefaction. Additional T2-weighted imaging at 21 months post-procedure (**J**) demonstrates a stable area of encephalomalacia (compared to **H**) but with further reduction of the central hypointense methemoglobin and hemosiderin (circumferential arrows), demonstrating further diminution of the CCM over a prolonged period.

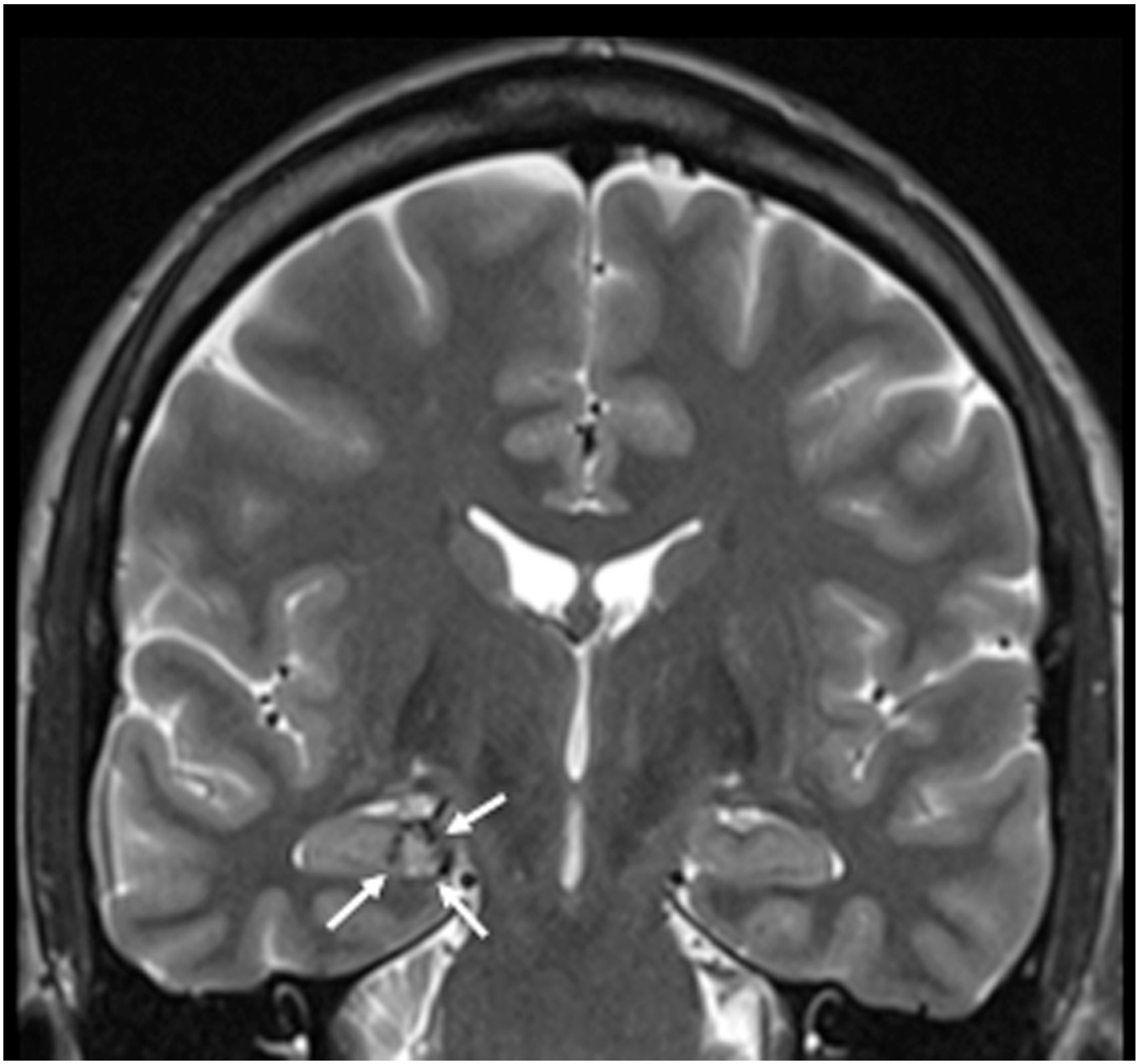

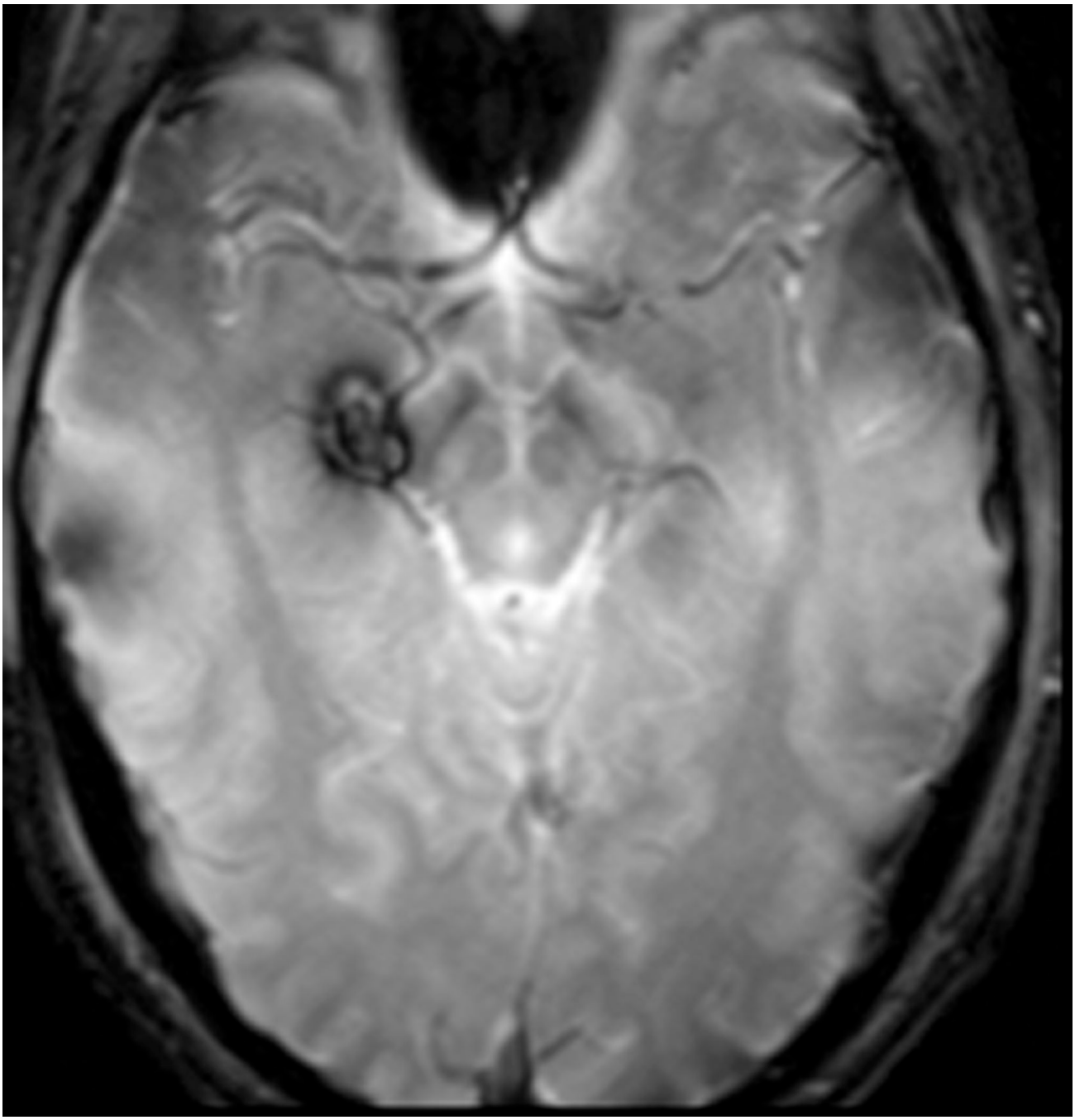

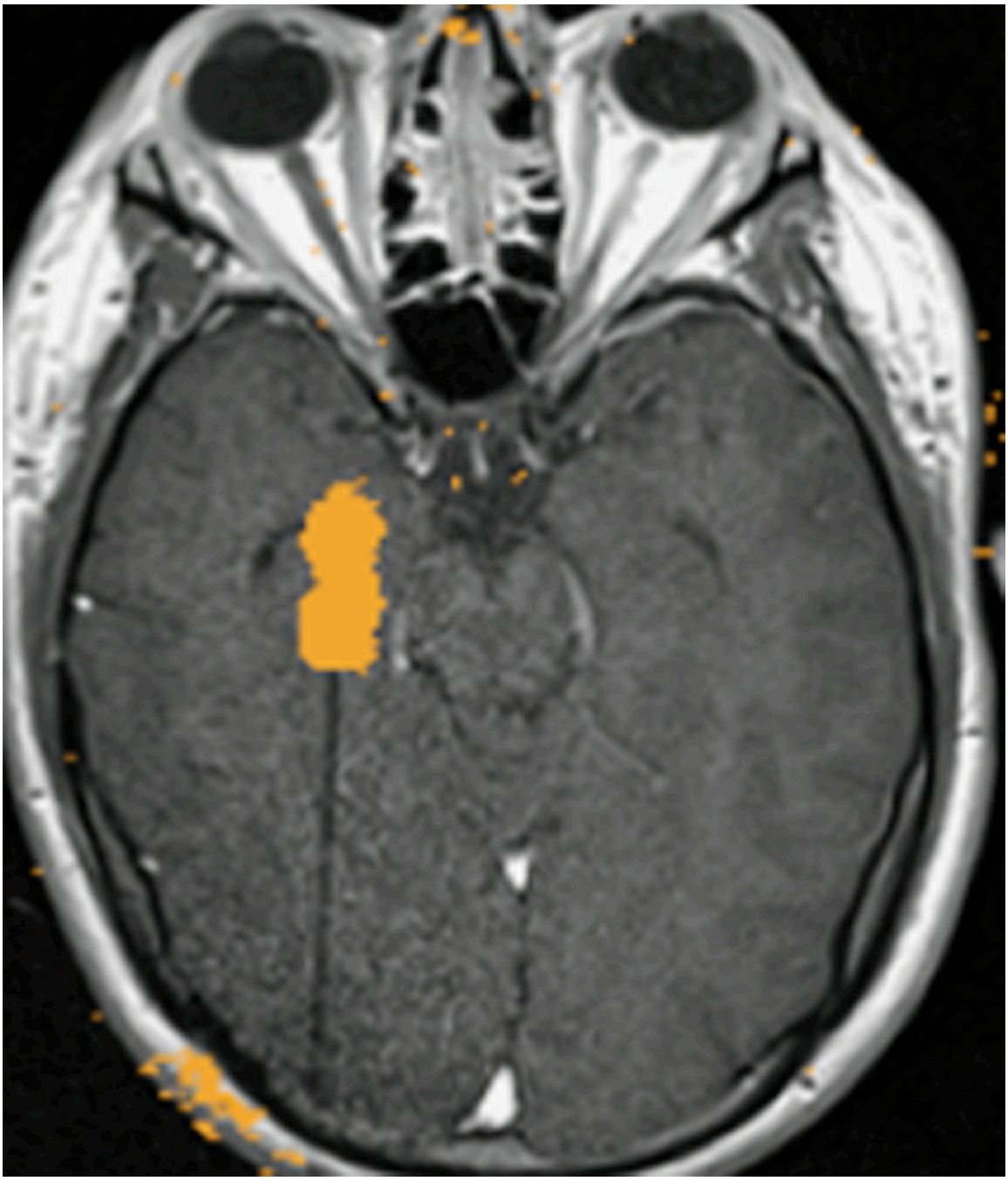

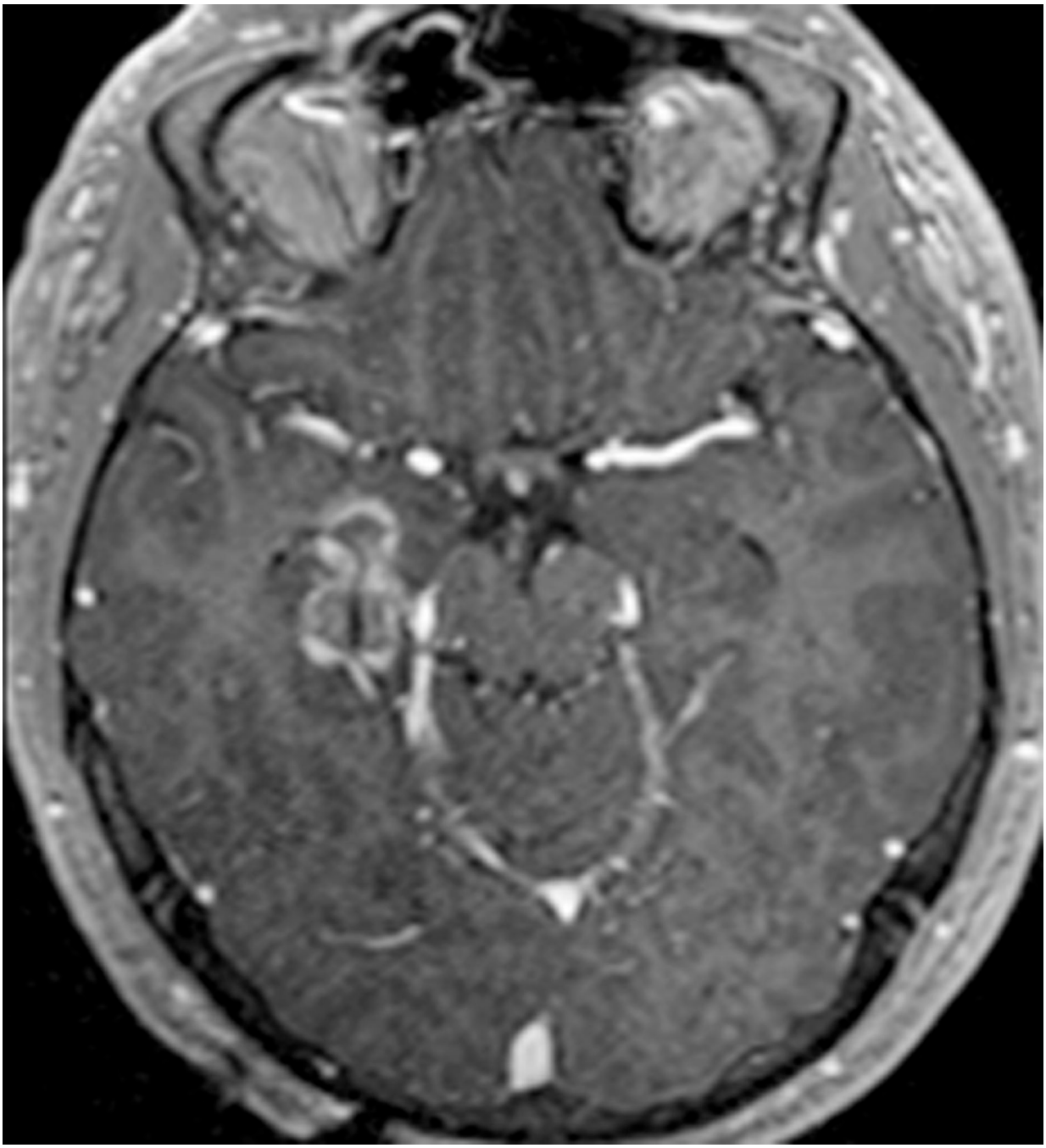

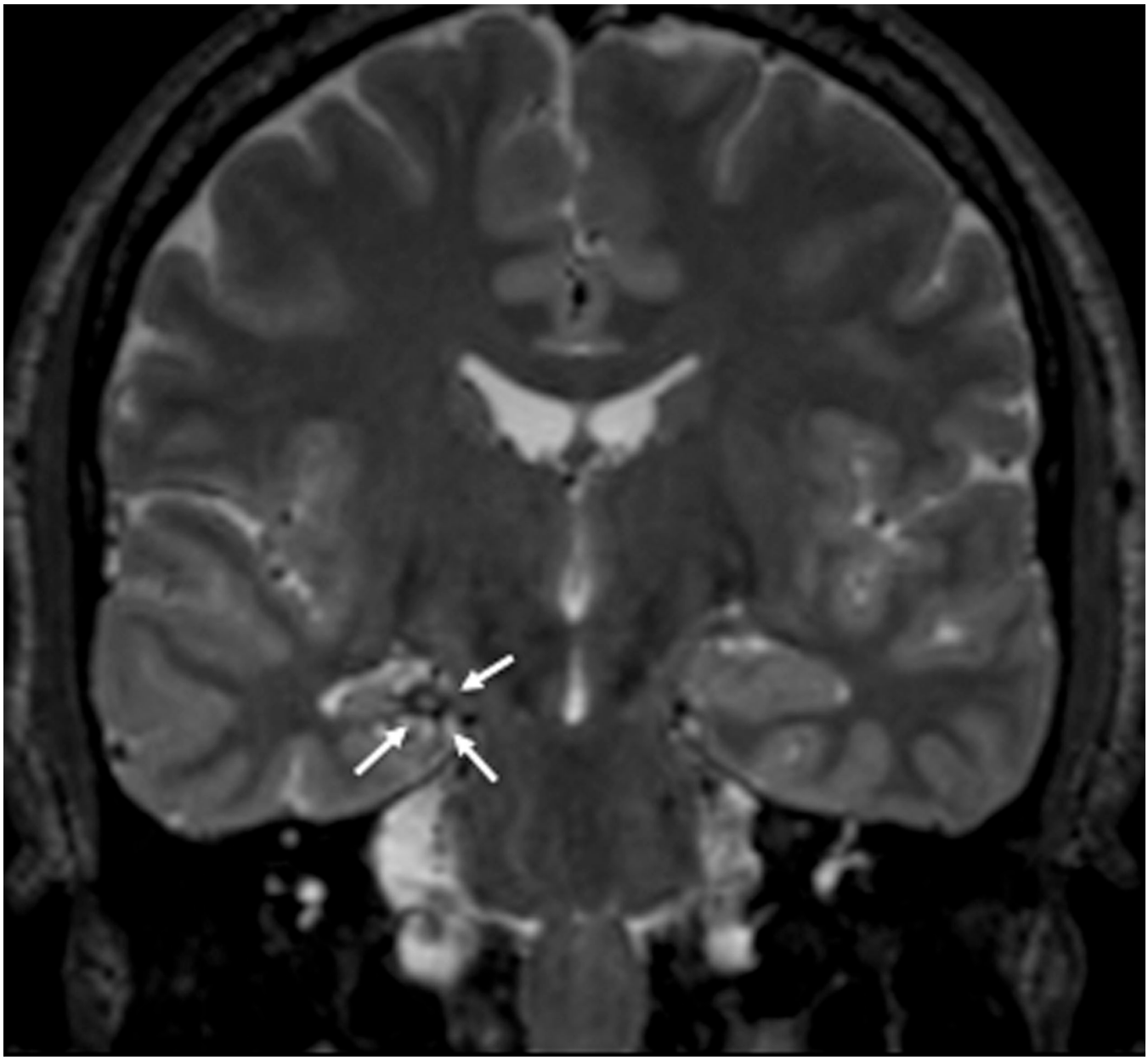

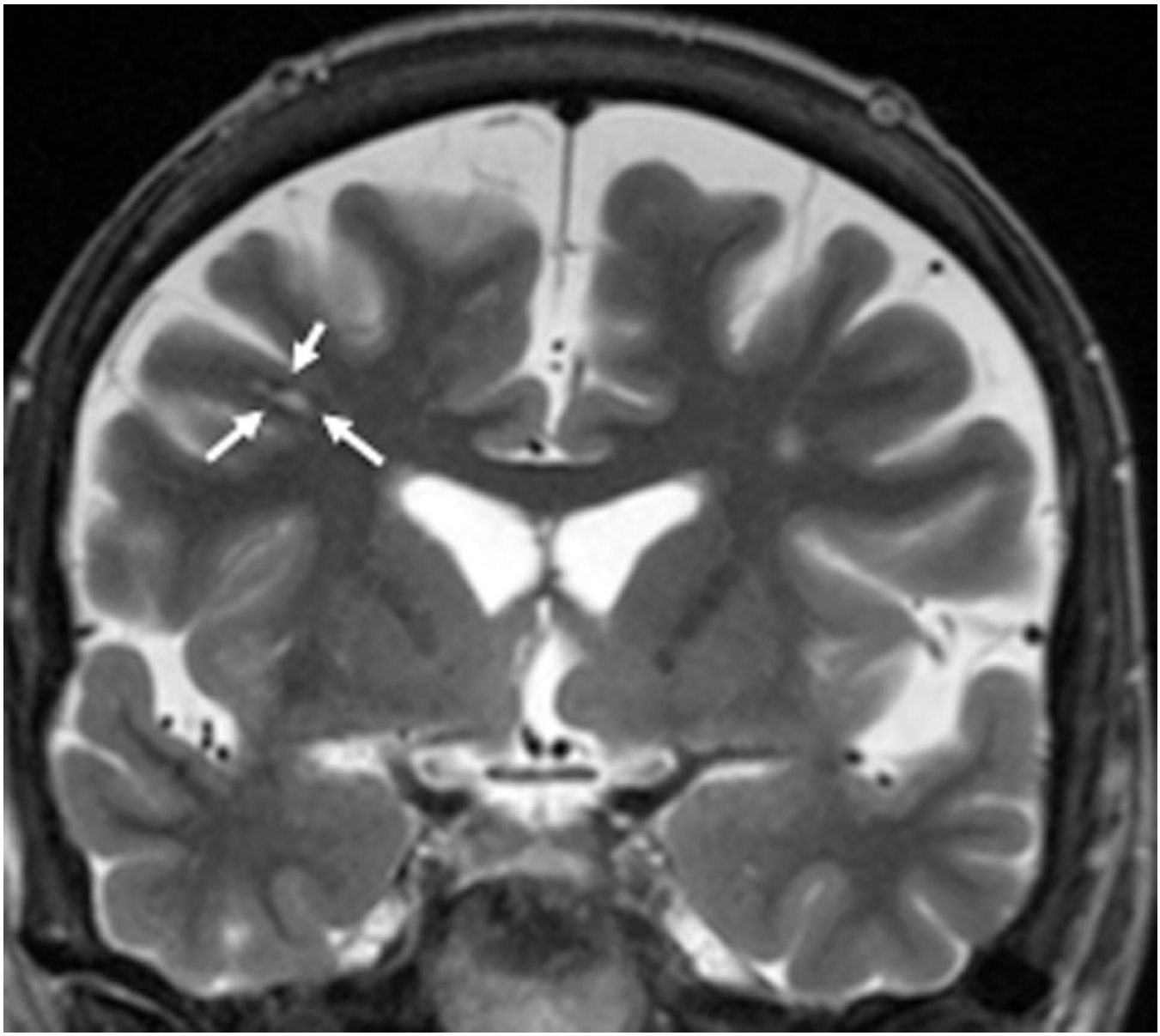

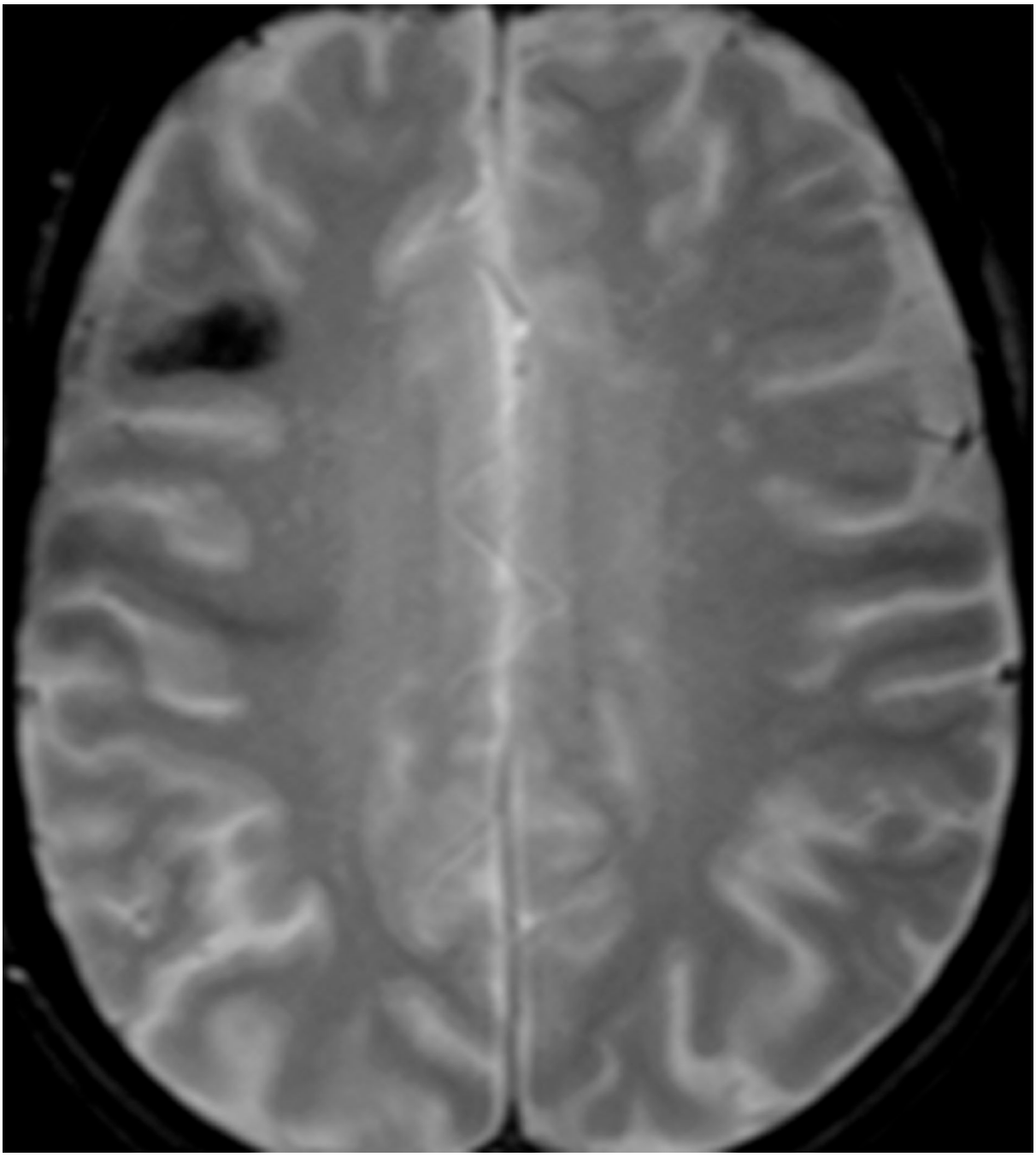

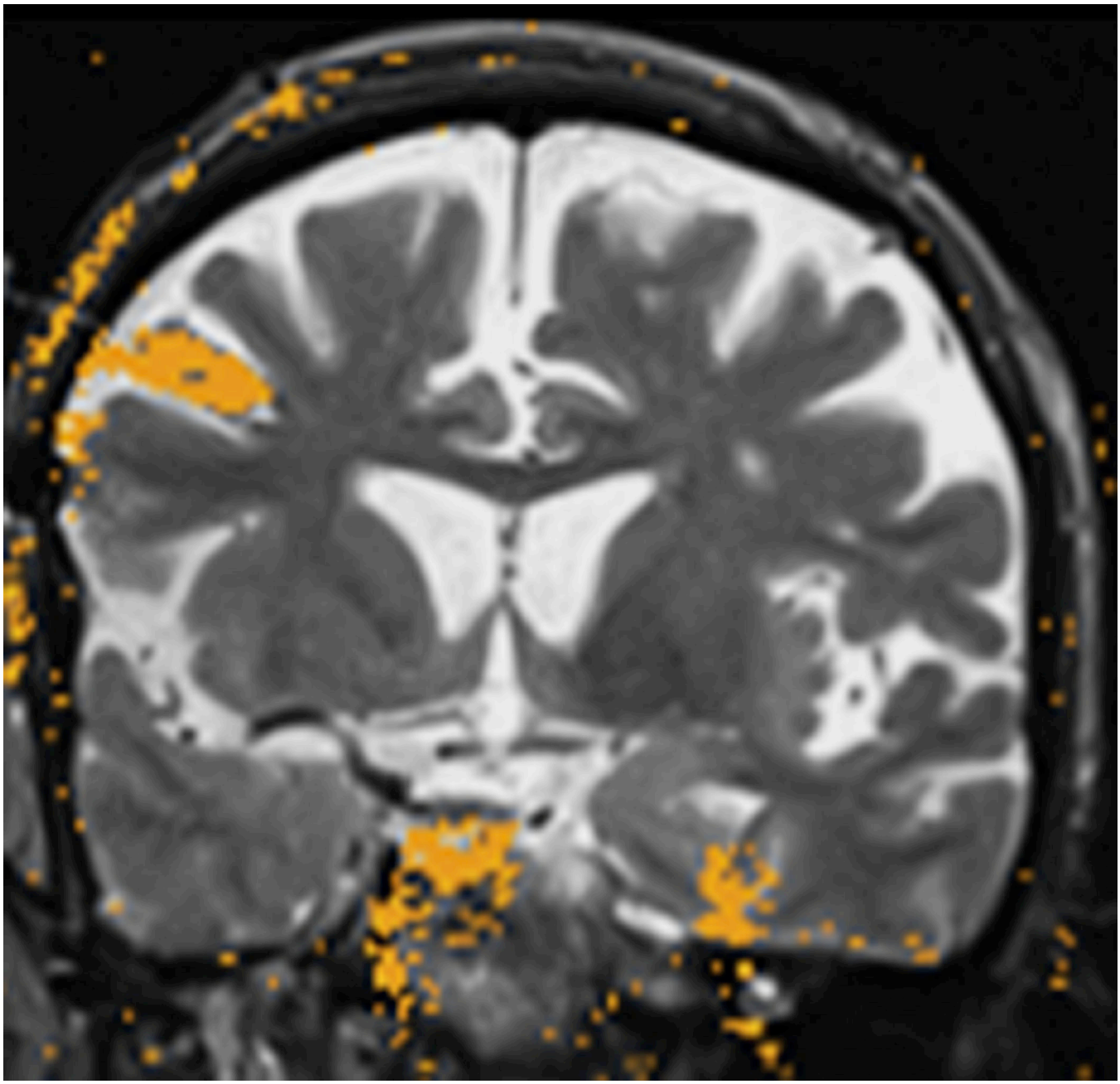

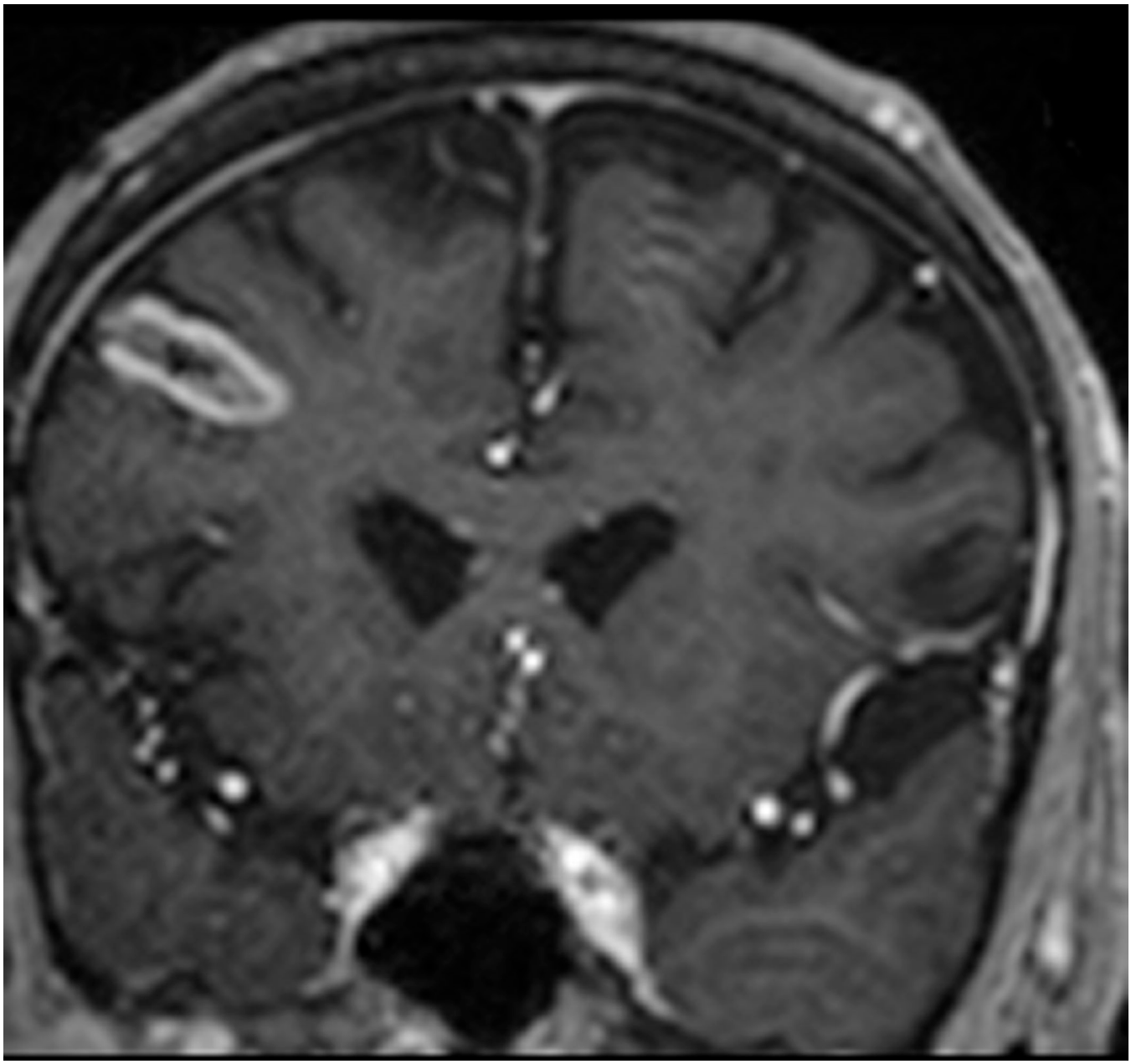

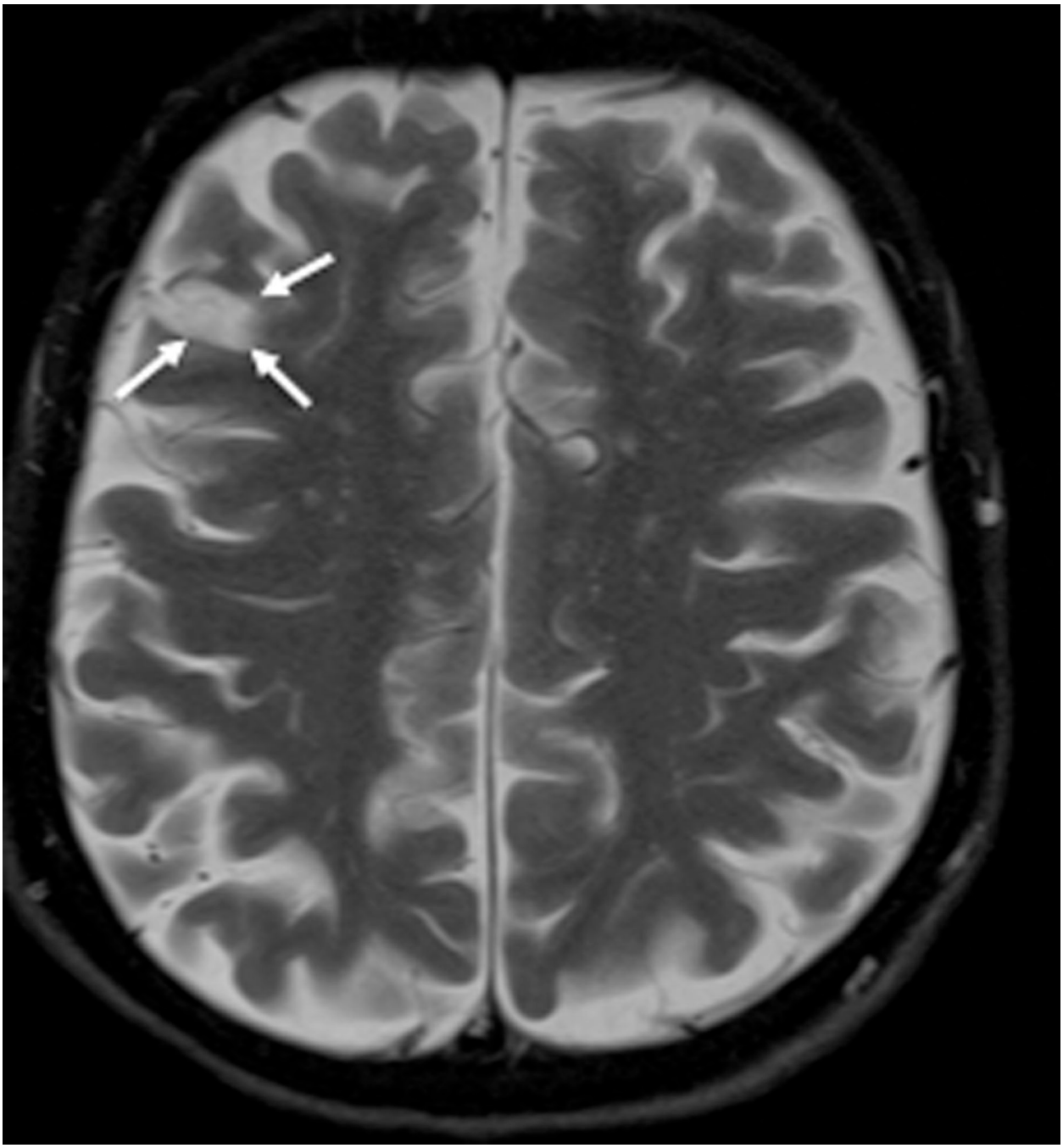

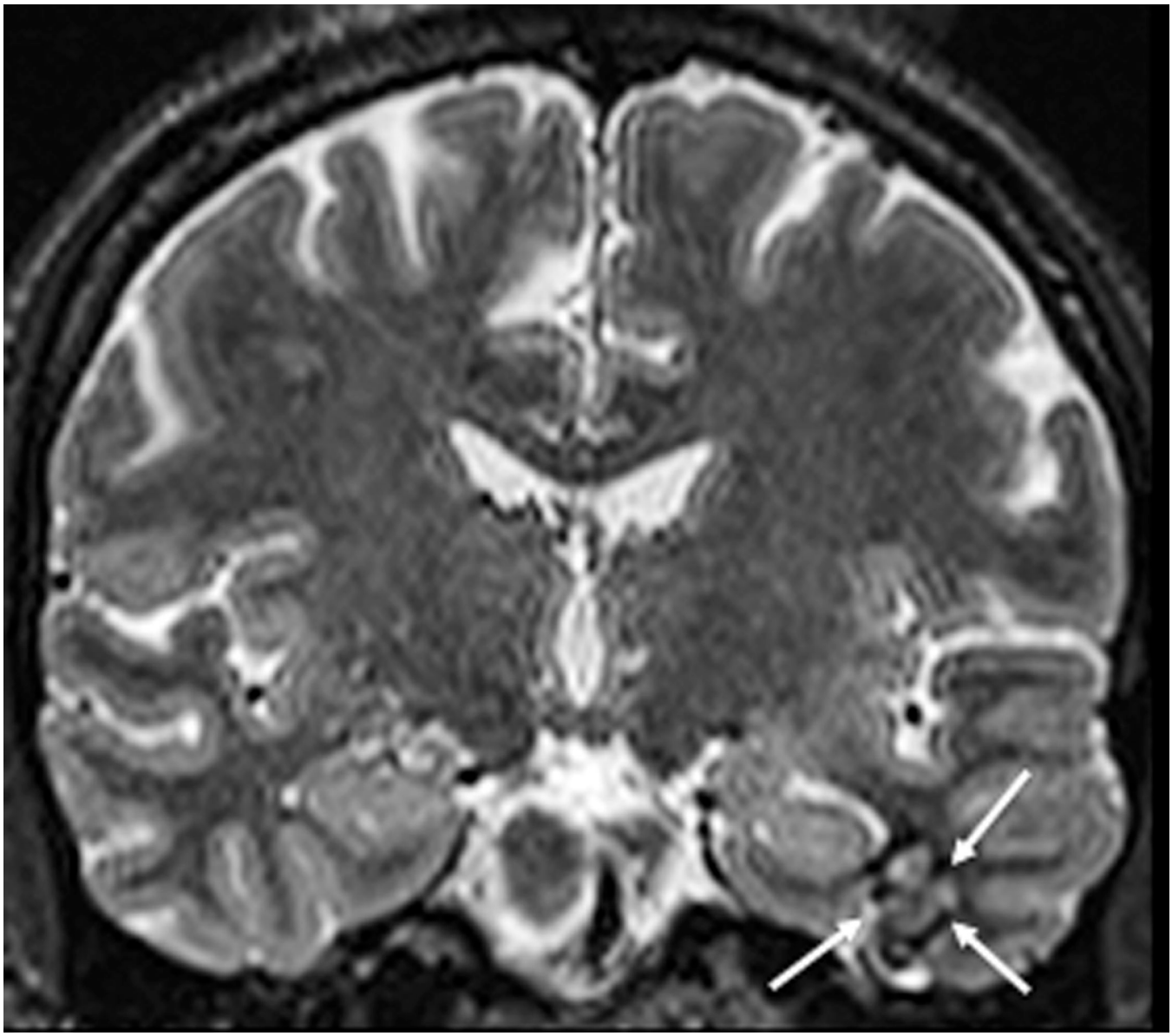

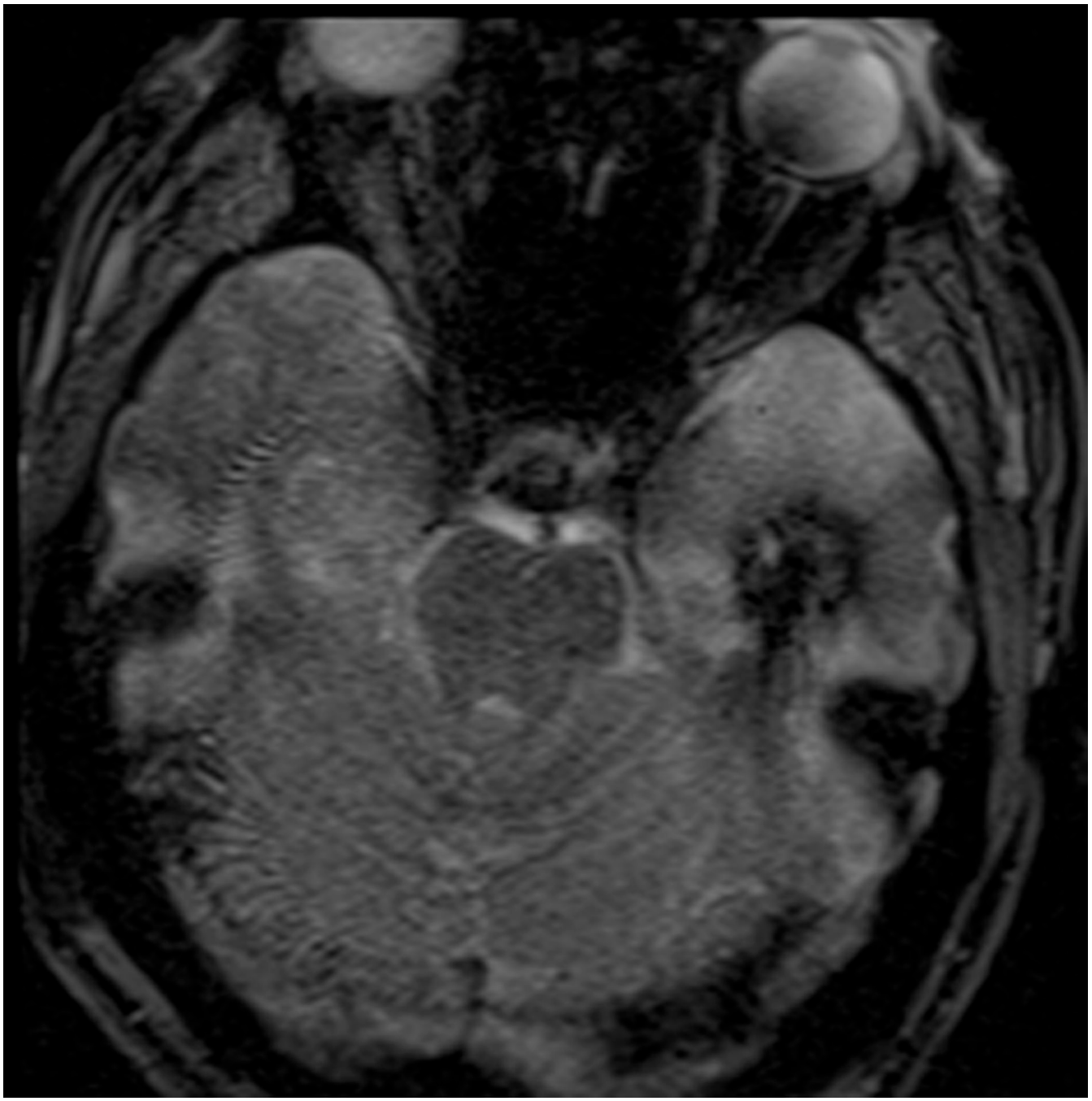

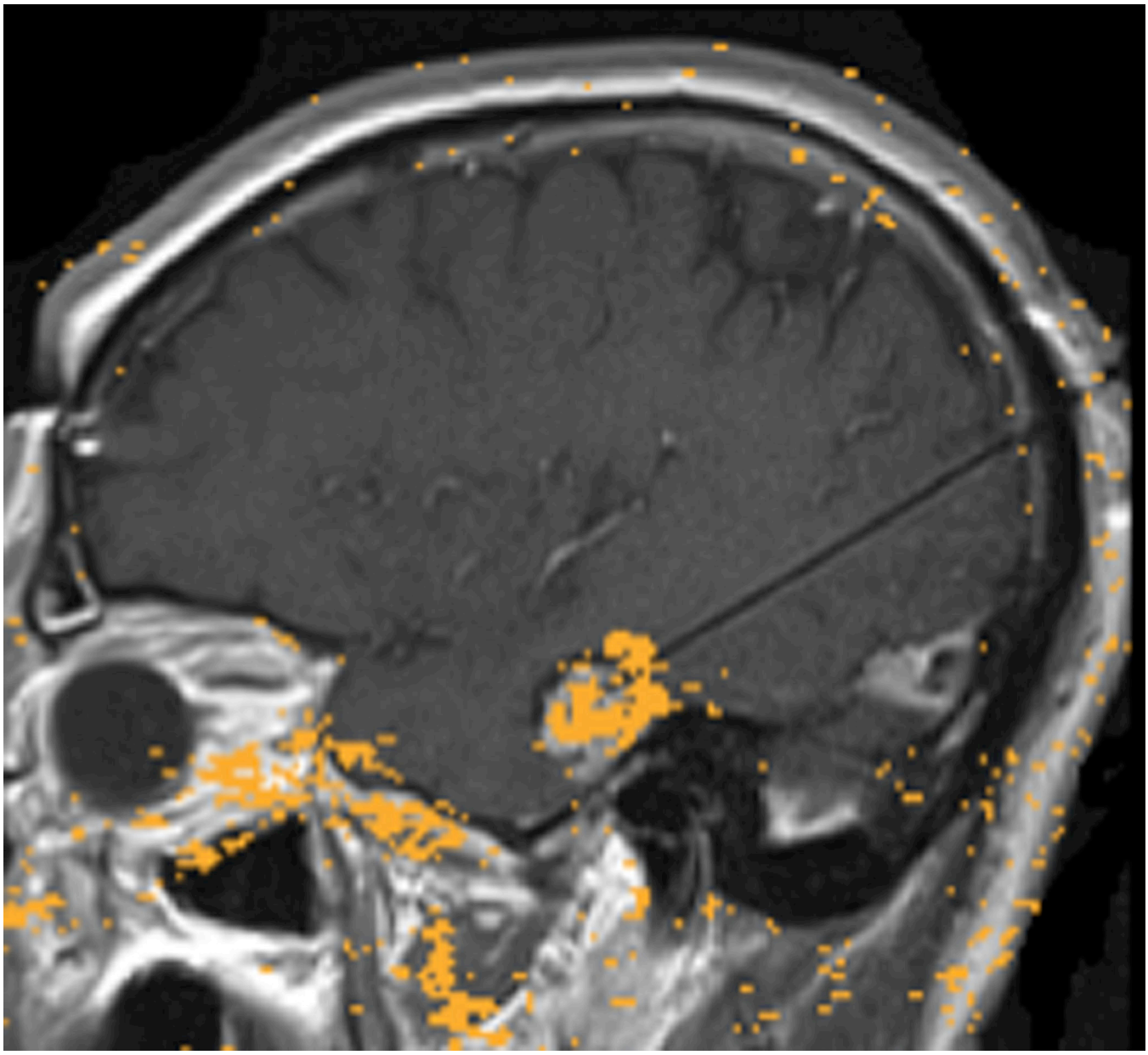

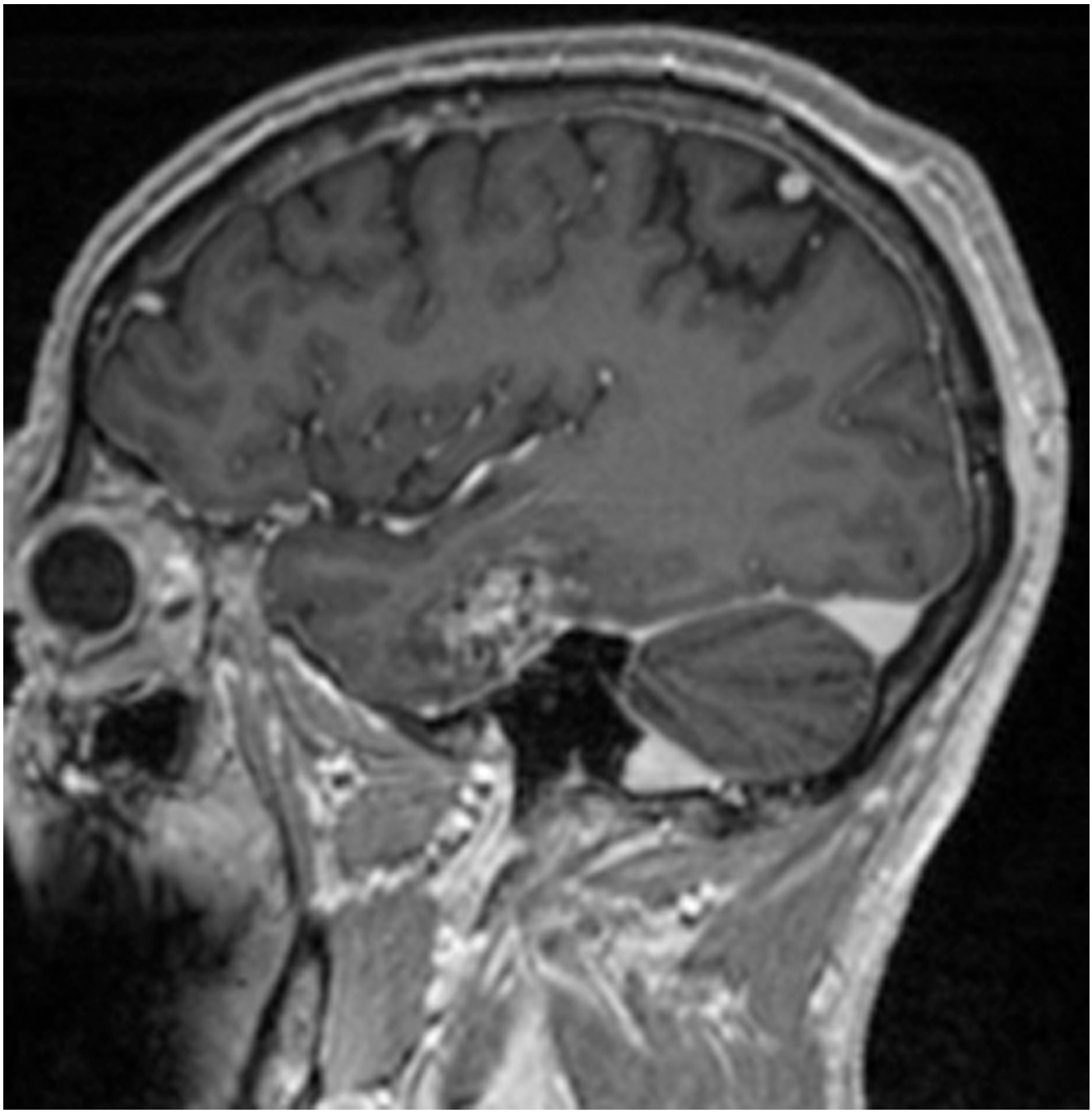

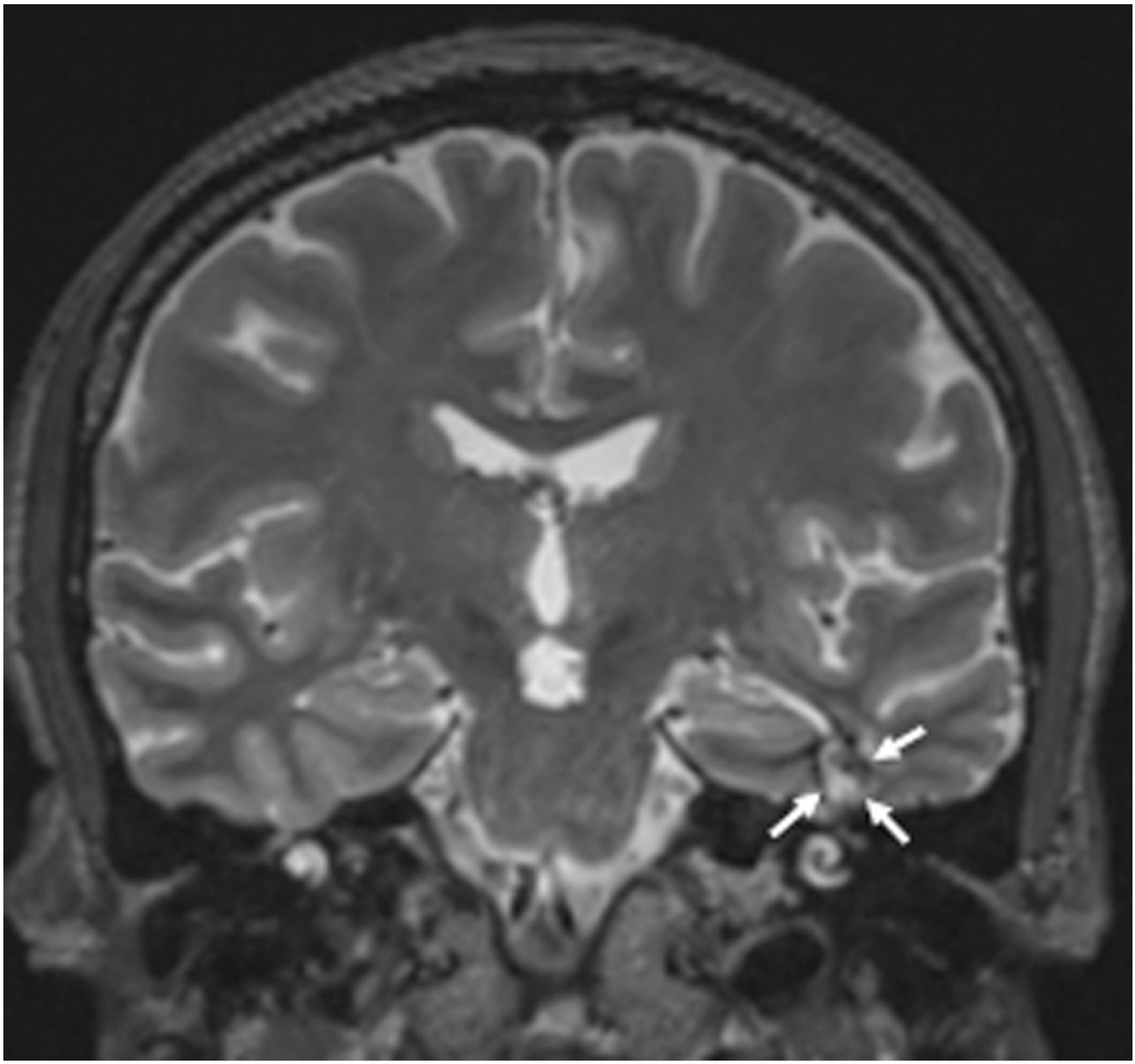

FIGURE 2. MRT-guided SLA of putative CCM associated with epilepsy in subjects 2 – 4

A–E, subject 2; **F–J**, subject 3; **K–O)**, subject 4. Preoperative coronal T2-weighted MR images (**A, F, K**) demonstrate lesions consistent with CCM (arrows) for each subject. Preoperative T2*-GRE weighted MR images (**B, G, L**) demonstrate susceptibility consistent with focal hemosiderin for each subject. Axial (**C**), coronal (**H**), and sagittal (**M**) brain tissue damage estimates (yellow pixilated regions of interest) generated by the laser workstation during ablation for each subject, with some evidence of GRE-based thermal signal dropout (lack of yellow pixels) impacting confluence of damage estimates. Note placement of stereotactic laser optical fibers in each case. Some thermal imaging artifacts (scattered yellow pixels) are also apparent near bone in some images. Immediate post-procedure

contrast-enhanced T1-weighted MR images in axial (**D**), coronal (**I**), and sagittal (**N**) orientations illustrate comparability of final acute ablation zones to previous tissue damage estimates. Remote post-ablation T2- weighted images in subject 2 at 12 months (**E**), subject 3 at 6 months (**J**) and subject 4 at 11 months (**O**), show ablated regions (arrows) to have small central regions of T2 hypointensity consistent with methemoglobin and localized surrounding hyperintensity consistent with liquefactive necrosis. These images suggest diminution of each CCM with surrounding encephalomalacia.

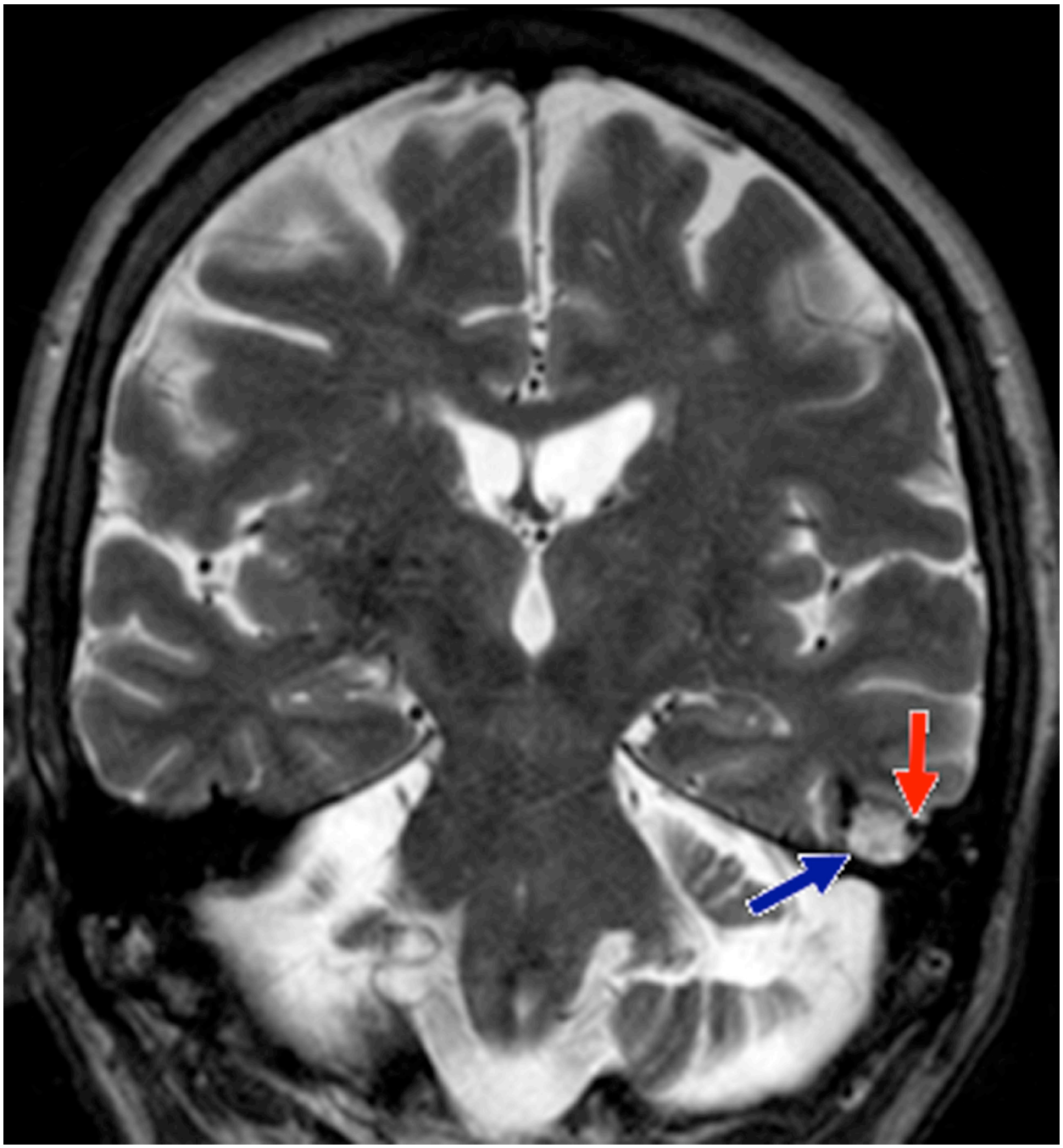

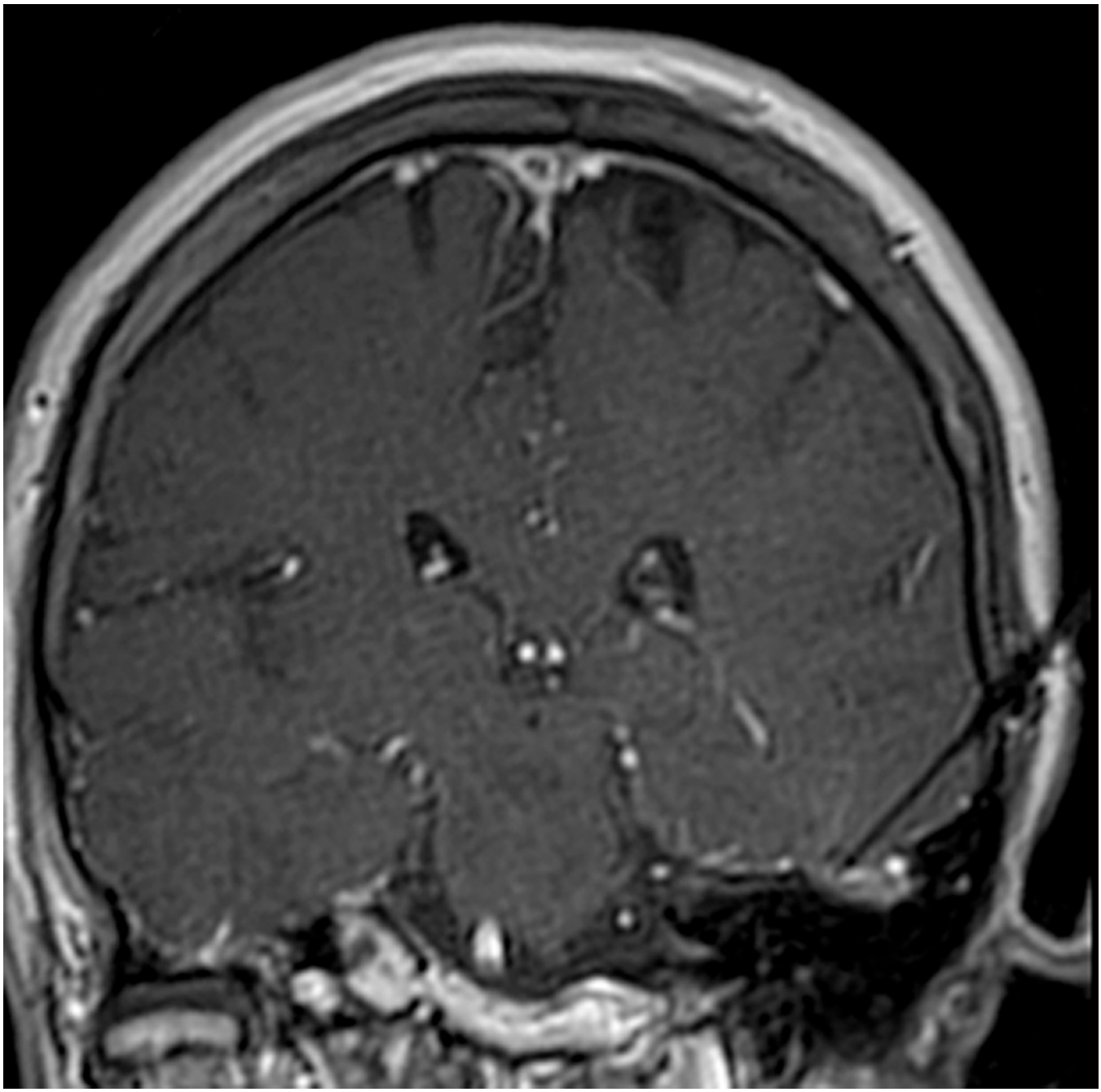

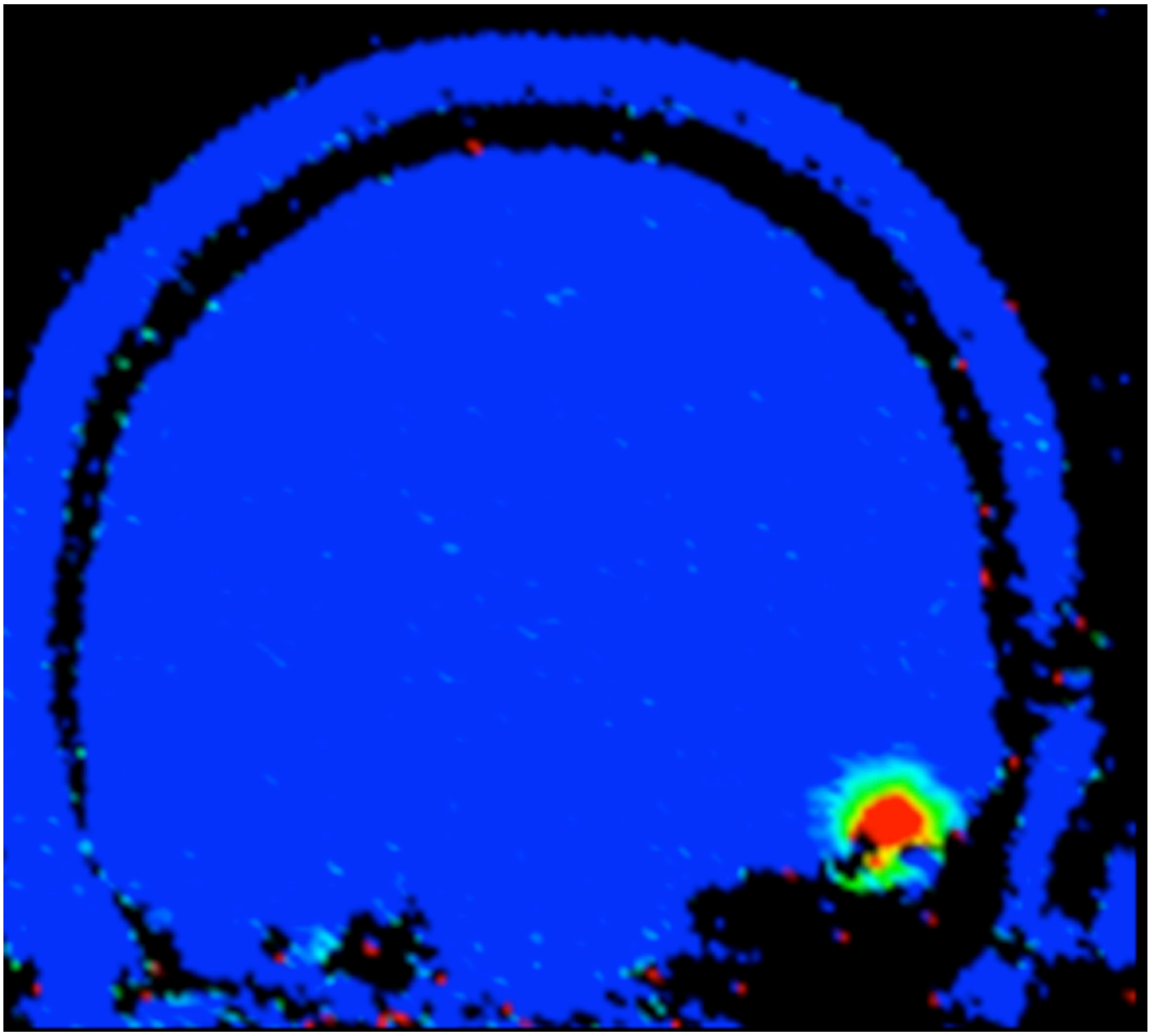

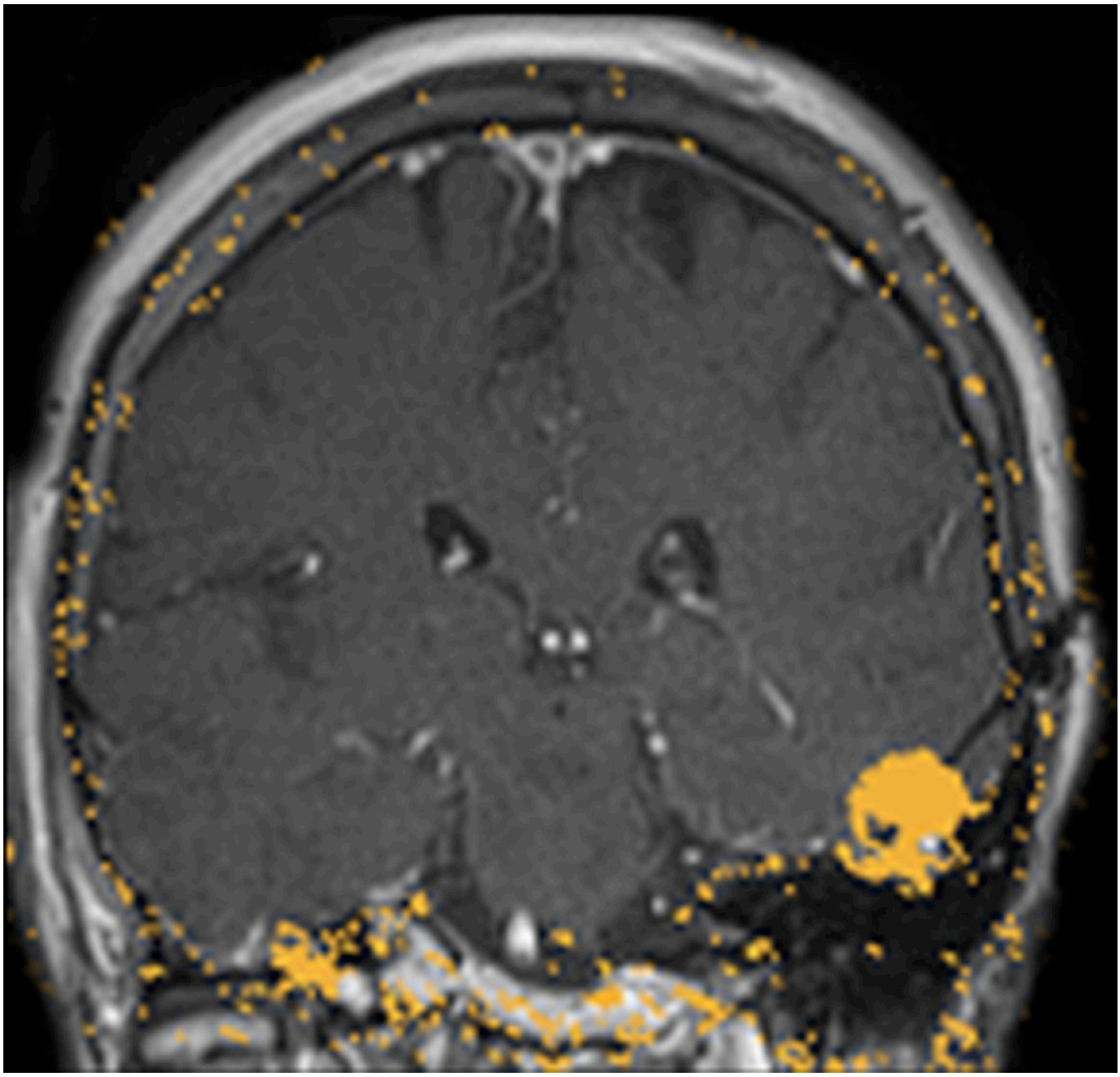

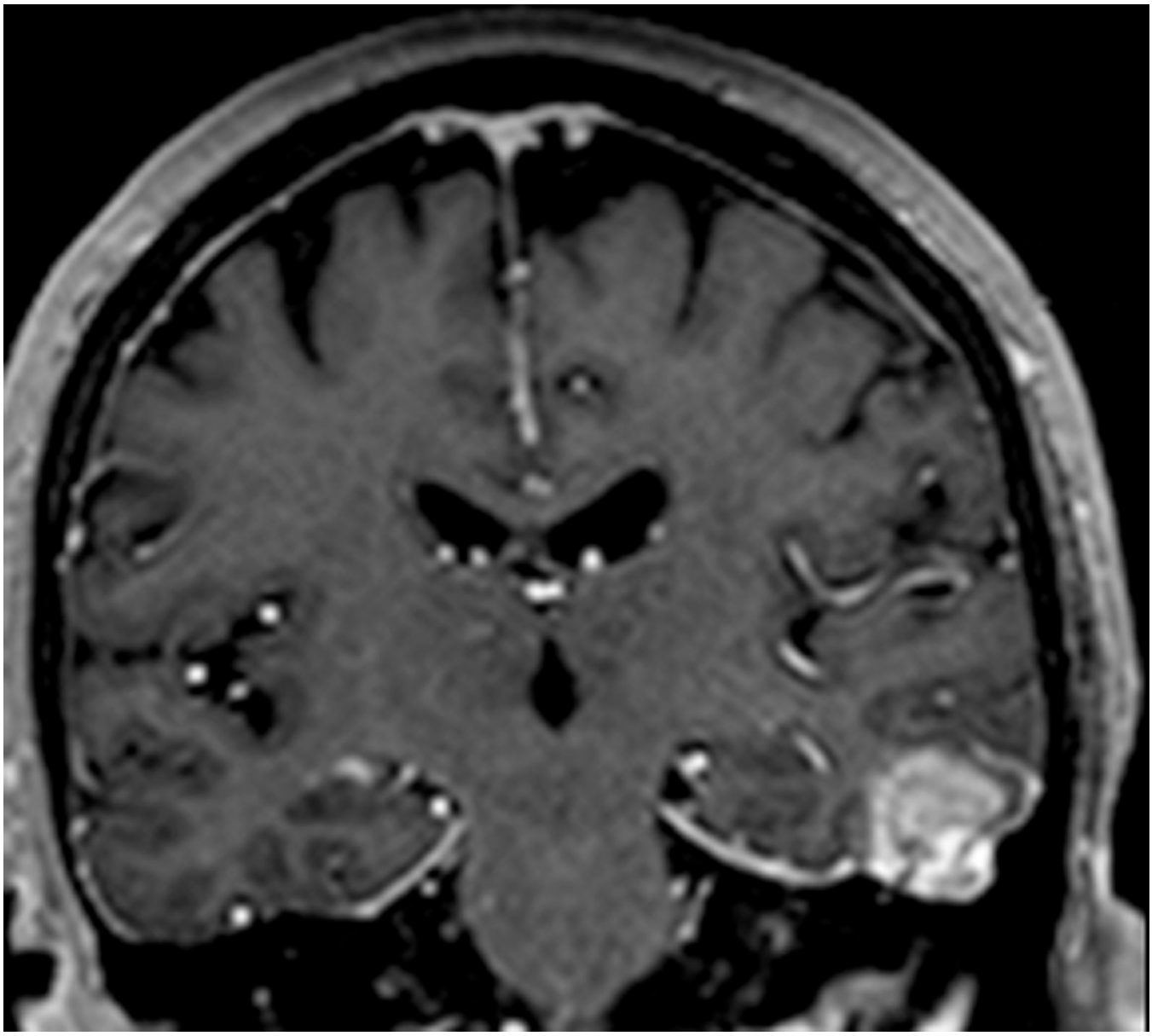

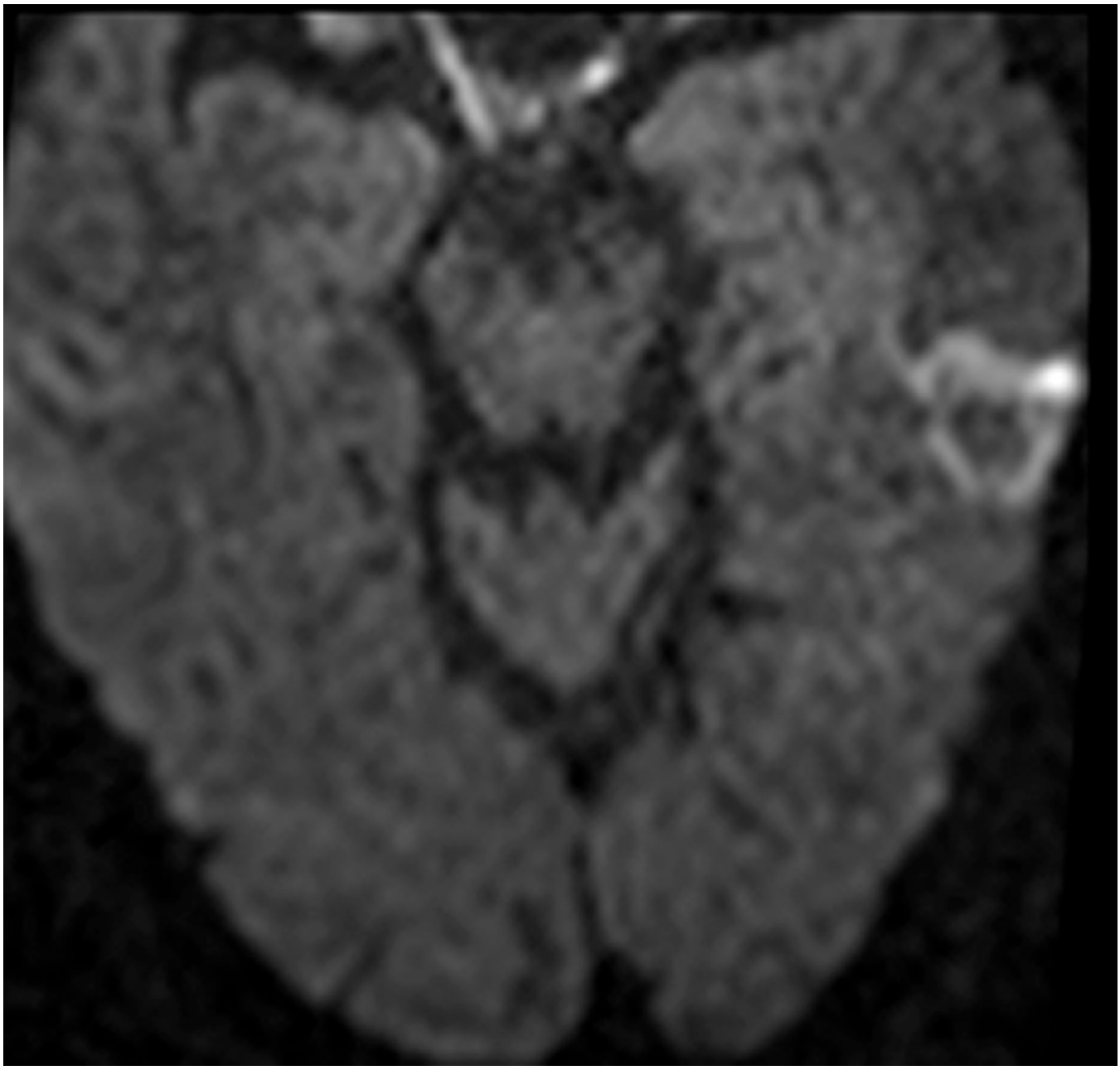

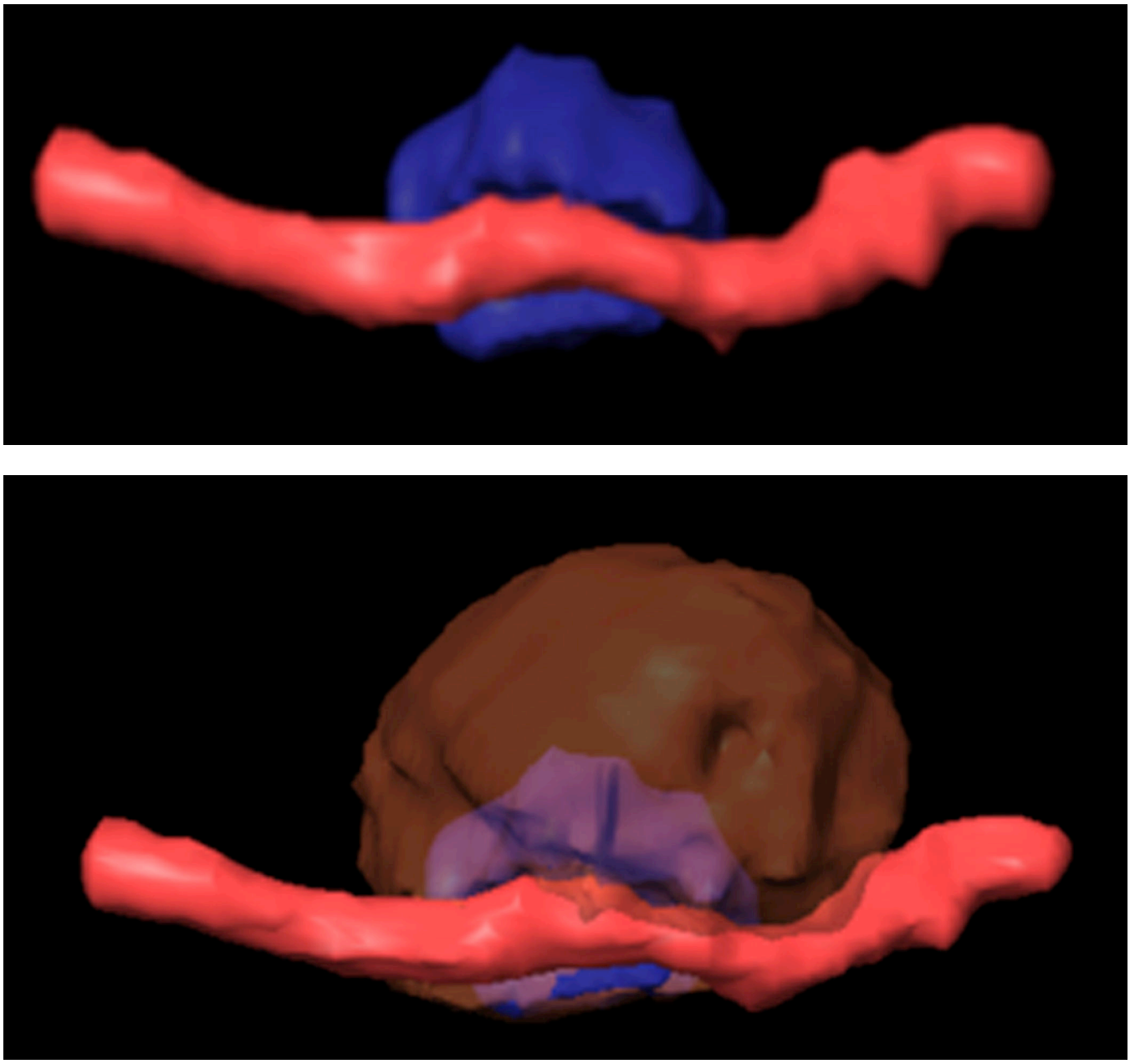

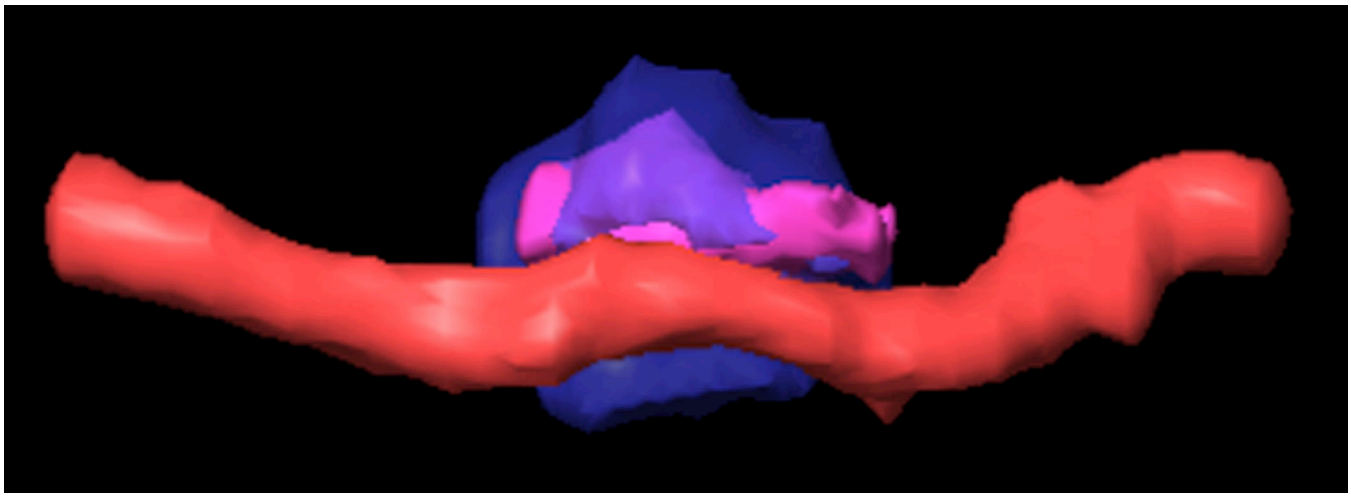

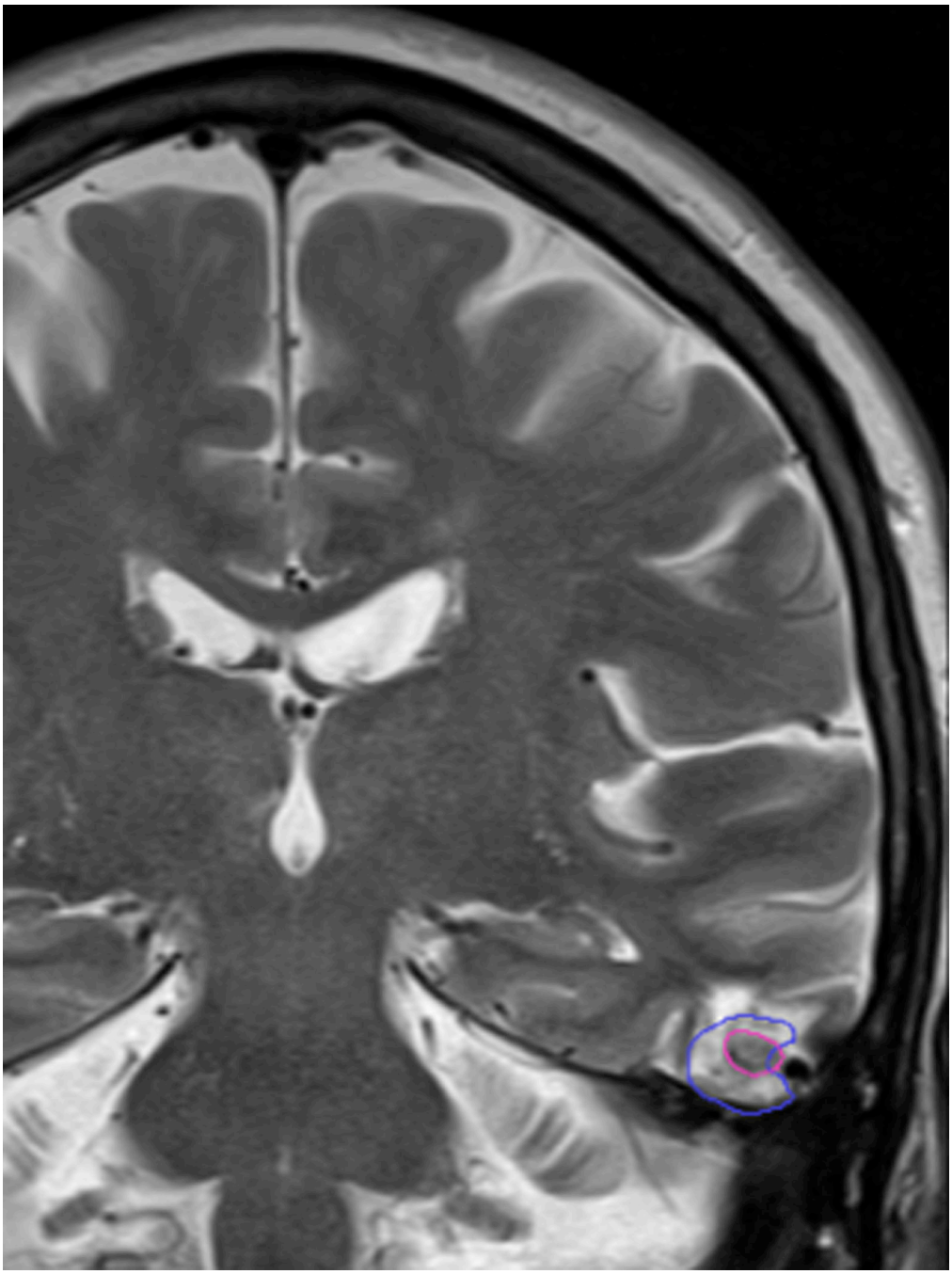

FIGURE 3. MRT-guided SLA in subject 5 ablates CCM while sparing an associated vein

A, Pre-operative coronal T2-weighted image exhibiting cavernous malformation (blue arrow) and adjacent vein of Labbé (red arrow). **B**, Intraoperative coronal T1-weighted image (residual contrast apparent) with fiber in place and lesion lacking contrast enhancement. **C**, Intraoperative coronal thermal imaging (with red=heat and blue=cold) as shown on the laser workstation during laser interstitial thermal therapy. Note absence of heating in the focal region of the vein of Labbé, as well as a small area of signal dropout inferomedially within the ablation zone corresponding to an area of increased methemoglobin imaged

preoperatively. **D**, Intraoperative coronal estimate of the total zone of irreversible laser ablation as shown on the laser workstation during therapy. **E**, Immediate post-procedure coronal post-contrast T1-weighted image confirming the ablation zone (area of enhancement). **F**, Preoperative axial T2-weighted image with cavernous malformation (blue arrow) and vein of Labbé (red arrow). **G,** Immediate post-procedure axial post-contrast T1-weighted image confirming the ablation zone (area of enhancement) and vein of Labbé. **H**, Immediate postprocedure diffusion weighted image confirming the ablation zone (area of diffusion restriction). **I**, Preoperative 3D reconstructions of the vein of Labbé (red) from preoperative post-contrast T1-weighted images in relation to the CCM (blue) from T2-weighted images. **J**, Immediate postprocedure 3D reconstructions of vein of Labbé (red) and ablation zone (yellow) from post-contrast T1-weighted images with superimposed preoperative CCM volume (blue). Note near complete overlap of ablation zone and CCM as well as lack of appreciable difference in diameter of the vein. **K**, 6-month post-procedure 3D reconstructions of the vein of Labbé (red) from post-contrast T1-weighted images, and residual CCM volume (magenta) from T2-weighted images, demonstrating diminution in size relative to the superimposed preoperative CCM volume (blue). **L**, 6-month postprocedure coronal T2-weighted image with outlined residual CCM (mangenta) and superimposed CCM outline (blue) from preoperative T2-weighted image illustrating lesion diminution.

Table 1

Demographic, Clinical, and Imaging Features of Patients with Epileptogenic CCM

Patient	Sex	Age (y)	Epilepsy duration (y)	Preoperative seizure type and frequency	Lesion location	Concordant MRI characteristics of CCM?*	Concordant hypo-metabolic focus on PET?	Concordant neurocognitive deficits?	Concordant seizure localization on long-term video EEG?
1	M	37	10	CPS; (2–7/month)	Left fusiform gyrus	Yes	Yes	(++) Moderate deficits in visual and auditory naming, and subtle deficits in verbal fluency, despite normal verbal memory: suggests left lateral TL involvement. (−) Visual memory deficits suggest right mesial TL.	Yes
2	M	28	4	CPS (1/day), rare secondary GTC; (1–2/month)	Right hippocampus	Yes	Yes	(++) Mild deficits in famous face recognition, emotional recognition, and aspects of verbal fluency are consistent with right anterior TL involvement (−) Lack of memory dysfunction suggests an absence of mesial TL dysfunction	Yes
3	F	66	21	CPS (1–2/week)	Right middle frontal gyrus	Yes, except shape atypically linear/gyriform	Yes	(+) Impaired attention and mild deficits in executive control processing suggest mild FL involvement	Yes
4	M	66	45	SPS, CPS, secondary GTC (1–2/month)	Left fusiform and inferior temporal gyri	Yes	Not obtained	(+) Mild deficits in auditory naming and moderate or greater deficits in semantic fluency, but otherwise normal language and memory function. Mild limitations in executive control processes	Not obtained
5	F	76	52	SPS and CPS (1–2/week)	Left inferior temporal gyrus	Yes +DVA	Yes	(++) Severe visual naming deficits in context of high average functioning	Yes

M, male; F, female; CPS, complex partial seizures; SPS, simple partial seizures; DVA, developmental venous anomaly; (++), findings strongly concordant; (+), findings modestly concordant; (−), some findings possibly discordant.

*1) T2 mixed intensity (“popcorn” appearance); 2) GRE/T2 peripheral hemosiderin ring ; 3) T2 lack of edema

Oper Neurosurg (Hagerstown). Author manuscript; available in PMC 2017 March 01.

Table 2

Outcomes of Stereotactic Laser Ablation for Epileptogenic CCM

Patient	Stereotactic method, approach	CCM Volume (cm^3)	Ablation Volume (cm^3)	Percent Lesion Ablated (%)	Adverse events	Last documented follow up (mo)	Seizure outcome after SLA	Comments
1	CRW, Temporal	0.36	0.91	80%	None	28	Engel 1A	
2	MRGF, Occipital	0.43	4.23	90%	None	19	Engel 1B	Aura at 4 mo. with medication reduction
3	MRGF, Frontal	0.22	1.89	94%	None	16	Engel 4B	ICM/resection at 9 mo → seizure-free
4	MRGF, Occipital	2.54	4.17	95%	None	12	Engel 1D	GTC at 9 mo with medication withdrawal and binge alcohol
5	CRW, Temporal	0.79	4.07	98%	None	12	Engel 1B	Seizure free except 2 SPS (brief difficulty speaking only) at 4 mo

CRW, Cosman-Roberts-Wells stereotactic frame (Integra, Inc.). MRGF, MRI guidance frame (ClearpointSmartFrame, MRI Interventions, Inc.). Engel Classification: 1A, completely seizure-free; 1B, nondisabling simple partial seizures only; 1D, generalized convulsions with medication withdrawal only; 4B, no appreciable change; ICM, intracranial electrode monitoring. Ablation volume represents the total amount of tissue ablated surrounding the original lesion, containing the either the CCM, hemosiderin ring, or surrounding tissue. Percent lesion ablated is the amount of original CCM that was included in the ablation volume, which was not always 100%.